University of California Transportation Center
UCTC Dissertation No. 151

Asymmetric Microscopic Driving Behavior Theory

Hwasoo Yeo
University of California, Berkeley
Fall 2008

Asymmetric Microscopic Driving Behavior Theory

by

Hwasoo Yeo

B.S. (Seoul National University) 1996
M.S. (University of California, Berkeley) 2004

A dissertation submitted in partial satisfaction of the

requirement for the degree of

Doctor of Philosophy

in

Engineering - Civil and Environmental Engineering

in the

Graduate Division

of the

University of California, Berkeley

Committee in charge:

Professor Alexander Skabardonis, Chair
Professor Carlos F. Daganzo
Professor John A. Rice

Fall 2008

The dissertation of Hwasoo Yeo is approved:

Chair _____ Date_____

_____ Date_____

_____ Date_____

University of California, Berkeley

Fall 2008

Asymmetric Microscopic Driving Behavior Theory

by

Hwasoo Yeo

ABSTRACT

Asymmetric Microscopic Driving Behavior Theory

By

Hwasoo Yeo

Doctor of Philosophy in Engineering – Civil and Environmental Engineering

University of California, Berkeley

Professor Alexander Skabardonis, Chair

Numerous theories on traffic have been developed as traffic congestion gains more and more interest in our daily life. To model traffic phenomena, many traffic theorists have adopted theories from other fields such as fluid mechanics and thermodynamics. However, their efforts to model the traffic at a microscopic level have not been successful yet. Therefore, to overcome the limitations of the existing theories we propose a microscopic asymmetric traffic theory based on analysis of individual vehicle trajectories. According to the proposed theory, vehicle traffic is classified into 5 phases: free flow, acceleration, deceleration, coasting, and stationary. The proposed theory suggests that traffic equilibrium exists as 2-dimensional area bounded by A-curve and D-curve, and explains phase transitions. The basic theory was extended to address driver behavior such as vehicle maneuvering error and anticipation. The proposed theory was applied to explain several traffic phenomena in congested traffic such as traffic hysteresis, capacity drop, stability, relaxation after lane change, and stop-and-go waves. We provided reasonable and intuitive explanations on these phenomena which cannot be easily understood with existing theories.

_____

Professor Alexander Skabardonis,

Committee Chair

ACKNOWLEDGEMENTS

I would like to express my thanks to the UC Berkeley professors for their endless supports and excellent teachings. I am indebted to my advisor Prof. Alexander Skabardonis for his guidance and support for my work, Prof. Carlos Daganzo for his great intuition and insight in transportation engineering, and Prof. Michael Cassidy for his advice and help in my work.

My friends in transportation engineering, Nikolas Geroliminis, Josh Pilachowski, Stella So, Offer Grembek, Juan Carlos Herrera, Anthony Patire and Ka-Fai Wong also deserve my thanks for their kind advices and cooperation during my stay in Berkeley. Finally I would like to give thanks to my Korean colleagues, Junho Lee, Kitae Jang, Kwangho Kim, Yoonjin Yoon and Koohong Chung.

To God who made the heaven and the earth,

My mother JungSook Kim, who made me,

And to my beloved wife SeungHyun Roh.

TABLE OF CONTENTS

LIST OF FIGURES

Chapter 1 Introduction

1.1 Introduction

Since the first studies on traffic characteristics and capacity (Greenshields, 1935) numerous theories on traffic have been developed as traffic congestion gains more and more interest in our daily life. To model traffic phenomena, many traffic theorists have adopted theories from other fields such as fluid mechanics and thermodynamics. These macroscopic modeling approaches have provided useful tools to understand traffic phenomena such as the formation and dissipation of traffic jams. They regard the traffic as fluid which follows the law of physics at all times. At a macroscopic level where roadway traffic is represented by variables of density (k), flow (q) and speed (v), fluid approximation approaches might be applied with reasonable relative accuracy. However, at a microscopic level, where individual vehicle behavior is of interest, the complicated driving behavior patterns observed in reality cannot be explained from the fluid mechanics' perspective. Therefore, improved microscopic traffic theories are needed to obtain a thorough understanding of driving behavior and related traffic phenomena.

Figure 1-1 shows flow-occupancy plots of detector data of a freeway. In free flow state, in which driving is not restricted by downstream traffic conditions, the flow (veh/hr) is

proportional to detector occupancy (% time) which can be regarded as a proxy value for density (veh/km). But beyond a certain critical value of occupancy, the flow decreases as occupancy (density) increases. This flow regime is called congested flow. In contrast to the free flow part, the congested regime shows "wide scattering" as shown in the diagrams.

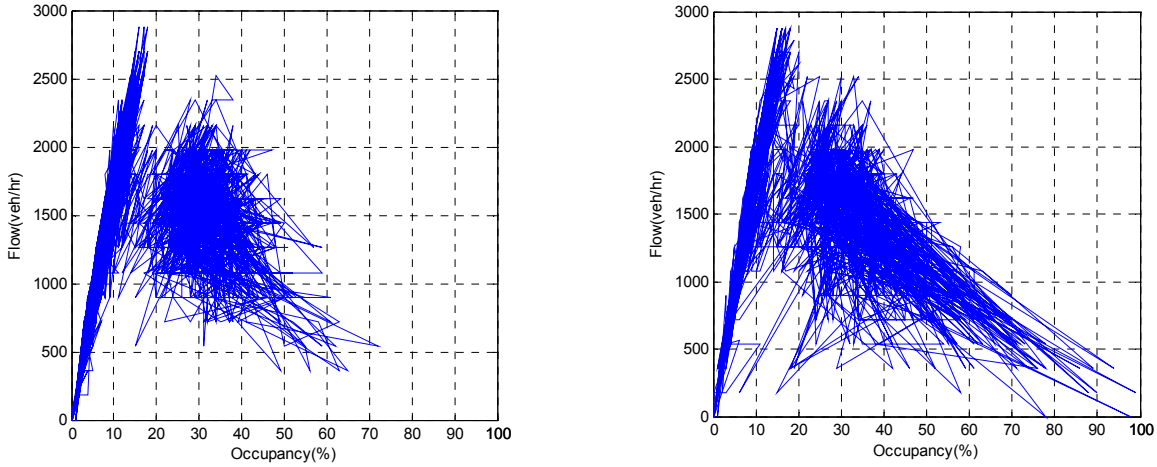

Figure 1-1 Flow-occupancy plot, 20sec data

The congested regime appears to be filled with complicated random events. Kerner and Rebhorn (1996b) mentioned such patterns in congested condition as "random transferences in all directions", and Koshi et al. (1983) as "extremely broad scattering". Looking at the data closely, we can find that actions in the congested parts are multi-directional as the former said. Even though the wide scattering can be partially explained by stochastic effect of drivers' difference in multi-lane and multi class situation, these actions cannot be easily understood with the macroscopic first order models such as LWR (Lighthill and Whitham, 1955; Richards, 1956). Until now, we don't have reliable theory which can explain the complicated actions in congested regime. And without a reliable theory, any microscopic simulation model cannot accurately predict the traffic conditions regardless of the number of the parameters used.

Brockfeld et al. (2003) tested 13 simulation models, and the results showed that the simulation errors in travel time for 6 km section highway were at least over 15% for all tested models. Including macro-simulation models like CA (Cellular Automata) and CT (Cell Transmission model; Daganzo, 1994, 1995), the test showed that the CT model is one of the best among 13 models. It means that current micro-simulation models cannot provide better results than macro-simulation. It is a serious challenge to the effectiveness of micro-simulation approach considering a lot of parameters and complex calibration process needed without improving results. Therefore, we need more accurate microscopic behavior theory which can overcome the current limit of the accuracy.

In most traffic theories, symmetry in acceleration and deceleration is assumed. In symmetry theories, acceleration process in congested part is done exactly in the opposite way of deceleration process in terms of fundamental variables of speed, flow and density. However, asymmetry in acceleration and deceleration has been observed by many researchers since 1950s. Newell (1965) published a theory that explained asymmetric behavior in acceleration and deceleration but even after Newell's initial theory, no empirical tests have been conducted and no alternative theory has been developed yet. It is partly due to the shortage of precise microscopic data because this asymmetry phenomenon cannot be easily observed in macroscopic data which are usually taken from time averaged detector data with time interval from 20 sec to 5min.

1.2 Driving Behavior

Driving behaviors can be represented by a set of rules describing actions which drivers take in response to driving situation and the situation change to achieve the purpose of the

trip. The driving situation is a collection of external factors outside of the vehicle-driver unit, and influence driver's vehicle-maneuvering actions. It includes (1) roadway geometry and conditions such as number of lanes, exit location, and pavement status, (2) inter-vehicle driving conditions such as speeds and distances of the surrounding vehicles, and weather conditions such as fog and rain.

Driver's behavior also can be understood in strategic level and tactical level. Strategic behavior is usually determined before the trip starts or far before the situation looms. Trip route, preferred travel lane and lane changing locations belong to this category. Tactical level driving behavior is determined in real-time. It includes optional lane changing to achieve faster running speed or to avoid a certain danger.

Roadway geometry and conditions are the main factors influencing strategic driving behavior. This behavior can be modeled using choice models such as route choice, lane choice model and mandatory lane changing choice model.

Inter-vehicle driving conditions determine the acceleration of vehicle, which can be represented by car-following models and optional lane changing choice model for passing. These models belong to the tactical level driving behavior.

Weather conditions influence both strategic level and tactical level driving behavior. Fog or heavy rain fall deters trip demand. In driving situation, they affect driver's lane choice in the strategic level, and cause larger gap and lower driving speed for safety's purpose. Therefore, car-following and lane changing behavior in adverse weather conditions are different from the ones without them.

Here, we assume that driving behavior has two components: (1) vehicle maneuvering behavior which is directly related to traffic flow, and (2) choice situation response.

1.2.1 Vehicle maneuvering behavior

Vehicle maneuvers can be classified into longitudinal and lateral movements. Longitudinal movement refers to the position change of a vehicle along a lane, and the lateral movement is the position change across a lane, which is perpendicular to the direction of longitudinal movement.

Longitudinal vehicle movement is always by means of car-following models in which every vehicle accelerates or decelerates so as to follow its leader while keeping a desired spacing. The latter is usually modeled as a function of the leader and follower speeds. In most car-following models acceleration is also a function of other environmental variables and driver's characteristics as in Equation (1-1).

$$a(t+\Delta t) = f(v_t^{lead}, v_t, gap_t \mid s^{jam}, \tau, ...) \tag{1-1}$$

Many car-following models have been developed in acceleration form as Equation (1-1). Also, distance form (Newell, 2002; Menendez and Daganzo, 2007; Yeo, et al., 2008) and speed form models (Daganzo, 2006) have been developed.

The environmental variables affect driver's behavior (decision), and they include current vehicle speed, speed of the lead vehicles and space gap to the lead vehicle. Driver-vehicle characteristics are the variables that explain the difference between drivers including vehicle length, jam spacing, reaction time, desired free flow speed and acceleration and deceleration.

The lateral movement can be represented by the lateral acceleration which is decided based on more vehicles than in longitudinal case. The environmental variables involved are the speed of the lead and lag vehicle in the neighboring target lane, and their gaps, and remaining distance to target location of lane change ($d_t^{t\_lane}$) and etc. The driver

characteristics are also preferred jam spacing in lane changing maneuvers and reaction time. Equation (1-2) shows the general form of the lateral movement function.

$$a^{lateral}(t+\Delta t) = f(v_t^{lead}, v_t^{lag}, v_t, gap_t^{lead}, gap_t^{lag}, d_t^{t\_lane} \mid s_{LC}^{jam}, \tau, ...) \quad (1\text{-}2)$$

1.2.2 Choice situation response

In addition to vehicle maneuvering behavior, we need choice models to explain how drivers respond diverse situations. For situations requiring decision, response can be represented as a probabilistic function as Equation (1-3). The probability of a certain action for a given situation is also a function of environmental variables and driver characteristics.

$$p^{action}(t+\Delta t \mid S) = f(v_t^{lead}, v_t^{lag}, v_t, gap_t^{lead}, gap_t^{lag}, d_t^{Exit}, ... \mid s^{jam}, \tau, ...) \quad (1\text{-}3)$$

There are three different categories of choice situations: a) destination-related situation such as mandatory lane changes to obtain the destination, b) faster-driving situation such as optional lane changes to increase speed or reduce travel time, c) safety-related situation including emergency braking, merging, weather, pavement situation. Although the classification above is object-based, sometimes, as in case of a lane selection model, one choice model can involve multiple situation categories.

There are also situations which change the driver characteristics which are supposed to remain constant during a trip. In weather situations such as rain or fog, drivers' behavior can be modeled by changing driver characteristic variables such as reaction time and jam spacing as follows:

$$\begin{aligned} &\tau(t+\Delta t \mid S) = f(v_t^{lead}, v_t, gap_t, d_t^{Exit}, S, ... \mid s^{jam}, \tau, ...) \\ &s^{jam}(t+\Delta t \mid S) = f(v_t^{lead}, v_t, gap_t, d_t^{Exit}, S, ... \mid s^{jam}, \tau, ...) \\ &... \end{aligned} \quad (1\text{-}4)$$

Although the change of driver's characteristics can be modeled in a deterministic way, it is preferable to use probabilistic choice functions because of the unpredictable nature of human driving.

1.3 Thesis Approach

The main purpose of the research is to provide a better understanding of the driving behavior. As a final goal in the extended research beyond this thesis, the driving behaviors can be modeled in the functional forms described in the previous section. In this thesis, as a practical starting point towards the goal, car-following and lane changing related issues are sought first.

This thesis is a part of the continuous traffic modeling research which has several steps illustrated in Figure 1-2. It starts from field observations on the traffic phenomena. We used a unique database of vehicle trajectories provided by the NGSIM program (NGSIM, 2006).

Based on these observations, we analyzed the data to find rules governing driving behavior, and aggregated found facts to build theories. For verification purpose, the developed base theories are applied to some traffic phenomena such as traffic stability, capacity drop and stop-and-go traffic, which are the most unexplained and controversial issues in traffic modeling.

After establishing theories with verifications, traffic modeling, simulation and application can be possible. In these stages, more data are required to extract parameters for simulation and evaluation of the performance. Even following the whole procedures suggested, the results of the application, which is on the top of the stages, cannot

completely replicate the reality. As illustrated, as the stage goes up, the matching power with reality goes down because of the "leak" between stages. Thus, any application of the theory to the real world must be used in a limited way. In this thesis, the upper stages from modeling to real world application are left for the future research.

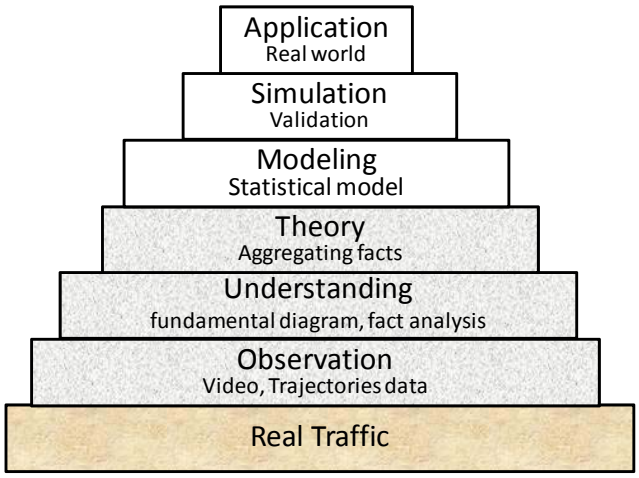

Figure 1-2 Traffic modeling

1.4 Thesis Organization

The thesis presents the development and application of a proposed microscopic traffic theory based on asymmetric driver behavior.

Chapter 2, "Previous Research", provides a short review on existing traffic flow theories, and discusses previous findings related to asymmetric driver behavior.

Chapter 3, "Asymmetric Microscopic Driving Behavior: Basic Theory", describes the proposed microscopic traffic theory. It provides a description on the data used, the fundamental concept of asymmetric theory with 5 traffic phases and phase transitions, and explains how drivers change traffic phase according to the driving situations.

Chapter 4, “Theory Extension: Human Driving Behavior”, presents extensions and refinements to the proposed asymmetric theory to address certain aspects of driver behavior, namely vehicle maneuvering errors and anticipation.

The proposed theory was applied to explain several observed phenomena in congested traffic. Chapter 5 presents the application of the theory on traffic hysteresis phenomenon, capacity drop, stability and relaxation after lane change. Chapter 6 provides an understanding and explanation of the stop-and-go phenomenon using the proposed theory.

Chapter 7, “Microscopic Fundamental Diagram”, presents an analytical form of the microscopic level fundamental diagram. A-curve and D-curve describing stationary relationship of speed and spacing are formulated. This Chapter also shows the relationship between A-curve and D-curve in diverse car-following situations.

Finally, Chapter 8 summarizes the major study findings and outlines future research directions.

Chapter 2 Previous Research

This chapter presents a brief overview on the traffic flow theory, and asymmetry-related research from earlier findings to recent car-following models that incorporate traffic oscillatory behavior.

2.1 Traffic Flow Theory

Traffic phenomena have been modeled as flow from the analogy between vehicular traffic and flow which is continuum. In this modeling method, the key variables are flow (q), density (k), and speed (v). These three variables have relationship of $q=kv$. In particular, the relationship between flow and density has been key modeling issues for long time. For the stationary flow, without lane change, the conservation equation holds:

$$\frac{\partial q}{\partial x}+\frac{\partial k}{\partial t}=0 \tag{2-1}$$

The fundamental relationship between flow (q) and density (k) was first proposed by Greenshields (1935). Since then, numerous models were proposed describing the q-k relationship. Also discontinuous models, in which congestion and free flow regime do not meet, were proposed like Koshi's model (1983). However, removing transition period and

extracting near-stationary conditions, Cassidy (1998) showed the existence of the continuous fundamental relationship of near-stationary flow.

LWR (Lighthill and Whitham, 1955; Richards, 1956) theory is the first order model for traffic dynamics. It has shown good agreements with experimental observations in congested traffic, but as a coarse representation of traffic, it cannot satisfactorily explain the mechanism of some traffic phenomena such as stop-and-go traffic. Daganzo (1997) pointed out the limitations of LWR model: (1) driver difference, (2) vehicular motion through shock, and (3) traffic instability. Recently, Nagel and Nelson (2005) pointed out the limitations of LWR theory in addressing 1) unstable flow, 2) spontaneous breakdown, 3) two-capacity phenomenon (or "capacity drop"; Banks, 1991).

To refine the dynamic traffic behaviors, a second order flow approximation model was first attempted by Payne (1971). Following the Payne model, a lot of second order models have been proposed. These models also assume fundamental relationship between speed and spacing which represents equilibrium flow. Helbing (1996) extended the Payne model using gas-kinematic equation. However, most of them were not successful in replicating real traffic phenomena as Daganzo (1999) criticized the second order flow approximations models.

Analyzing aggregate detector data, Kerner (Kerner and Rehborn, 1996a, 1996b, 1999; Kerner, 2004) has developed a three-phase traffic theory. He classified traffic into 3 phases: free flow, synchronized flow, and wide moving jam. He tried to explain spatial-temporal traffic patterns using transitions between these three phases. In three phase theory, "synchronized flow" is characterized by the fixed location of downstream front at a bottleneck, while the front of "wide moving jam" moves upstream with constant

velocity. “Synchronized flow” can be compared with the normal congested traffic, and the “wide moving jam” is “stop-and-go” waves inside congestion. Although he was not the first, he pointed out two empirical phenomena: (1) synchronization of average speed between different freeway lanes and (2) wide spreading of empirical data in flow-density plane. From these perspectives, Kerner concluded that there does not exist any fundamental relationship in congested region. Instead, the “synchronized flow” covers the 2-dimensional area of flow-density relation. However, as a qualitative approach, he provided only the classification of the traffic phases, and did not provide exact behavior inside the “synchronized flow” and the procedures how the transitions between traffic phases are made. However, in the fundamental diagram approach that Kerner seriously opposed, the stochastic nature of traffic and transitions between phases can partly explain the wide scattering in flow-density plane. Furthermore, diverse situation of traffic such as lane changing, merging and diverging also contribute to the wide scattering. For example, in multilane freeway, lane changes can cause speed synchronization. Therefore, the two phenomena Kerner pointed are not unique features of three-phase theory, and can also be understood in fundamental diagram perspectives.

2.2 Earlier Findings on Asymmetric Behavior

Regardless of the order of differential equations used, most theories from fluid mechanics have assumed symmetry in acceleration and deceleration. However, different from material flow, driving behavior cannot be perfectly symmetric.

The asymmetry in vehicle’s acceleration and deceleration has been observed by several researchers since the 1960’s. The first traffic observations related to

acceleration-deceleration asymmetry was obtained by Forbes (1965), Foote (1965), and Edie (1965). Forbes (1965) noticed that the driver's response is slower in acceleration than in deceleration. From three-car experiments, he noted that the driver response times in and out of a slowdown have following relationship:

t_h (out) $\approx 2t_h$ (in). (2-2)

Figure 2-1 shows diverse driver response times by Forbes (1965), which shows the impact of response time on traffic flow. Response time and flow show negative relationship. With higher response time, accelerating vehicles recovering from a slowdown have lower flow.

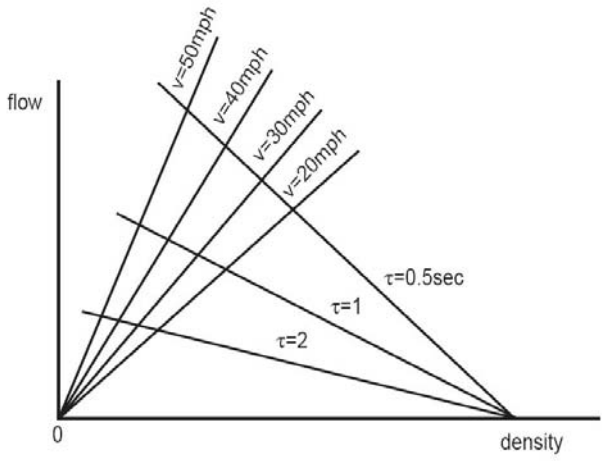

Figure 2-1 Response time from Forbes (1965)

Foote (1965) observed traffic data obtained in tunnels. Dividing platoons into three types: constant speed, accelerating and decelerating, he traced the platoons, and found that decelerating vehicles have higher flow for given speed than the other types of platoon. This phenomenon was observed in all three tunnel sites, and he could obtain time headway (t_h)-speed (s in feet/sec) relations as follows:

Acceleration time headway: $t_h = 1.6 + 35/s$ (sec) (2-3)

Constant speed time headway: $t_h = 1.6 + 25/s$ (sec) (2-4)

Deceleration time headway: $t_h = 1.1 + 30/s$ (sec) (2-5)

Edie (1965) investigated platoon behaviors using analyzed data from aerial photos taken in 6 seconds interval. His study site is one lane of the George Washington Bridge which was not affected by lane changing behaviors. Figure 2-2 (a) shows the flow-concentration (density) plots of a 13-vehicle platoon for 30 seconds. As in the Figure, we can find clockwise movement in flow-density plane. By tracing platoons of 5-6 vehicles, Edie also obtained Figure 2-2(b). A compressing platoon, which is in deceleration, has higher flow for given speed than an expanding platoon in acceleration. The separation of acceleration and deceleration in flow-density plane can be clearly seen in the plots.

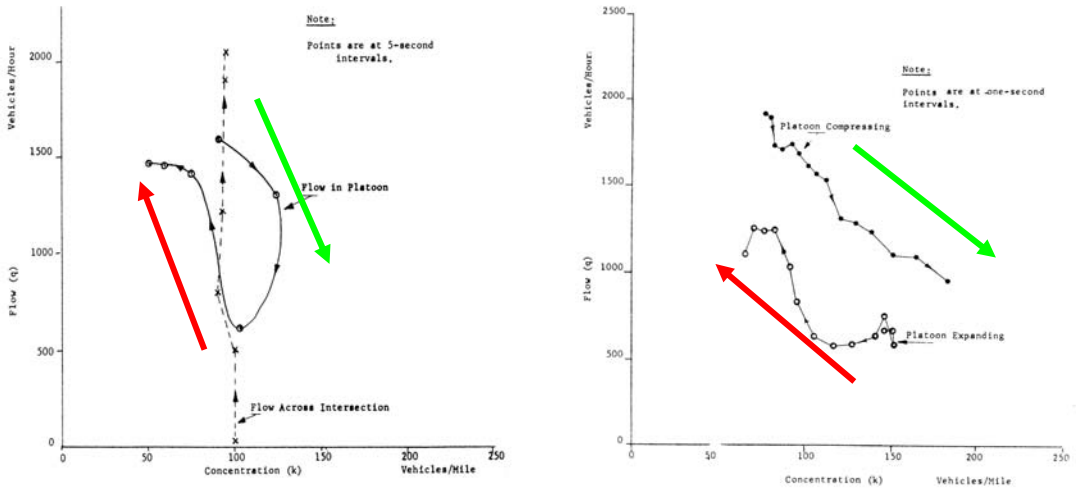

(a) (b)

Figure 2-2 Edie's observations (1965)

It was Newell (1965) who first provided a theoretical explanation on this phenomenon.

Based on the observations showing asymmetric behavior by Forbes, Foote, and Edie, Newell suggested two separate curves for acceleration and deceleration in congested traffic as shown in Figure 2-3. As illustrated in the Figure, the spacing in acceleration is always larger than the one in deceleration for the same speed. This asymmetry in acceleration-deceleration forms a clockwise loop in flow-density plane like Edie's (1965) results shown. Different from Forbes (1965) who noticed only response time change and assumed same jam density, Newell used different jam spacing d_0, d_1 for deceleration and acceleration respectively. He also ascribed the cause of traffic instability allowing the growth of a small perturbation, to the wave speed difference inherent from the asymmetry.

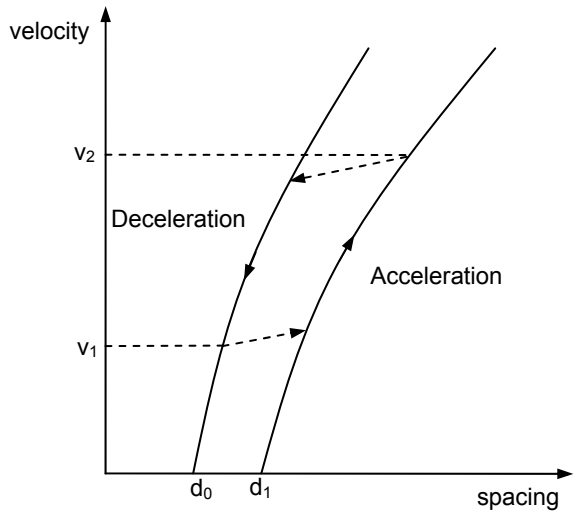

Figure 2-3 Newell's two-curve theory in congested traffic

Using vehicle trajectory data obtained from aerial photos, Treiterer and Myers (1974) named the loop forming movement in the flow-density plane as "Traffic hysteresis phenomenon". Basically, their finding is not different from the previous ones by Foote (1965) and Edie (1965) and the Newell's theory (1965). They also thought the hysteresis

loop was the result of asymmetry in acceleration and deceleration. A detailed discussion and explanation on the "Traffic hysteresis phenomenon" is provided in Chapter 5.

Koshi et al. (1983) suggested "reverse-λ" shape flow-density relationship (Figure 2-4 (a)) from test car experiments. It implies a discontinuity between free flow region and congested region. In their experiment, they also noted asymmetric behavior. Plotting speed-clearance (gap), they showed that acceleration (≥ 0.1g), deceleration (≤ -0.1g), and steady run are not on the same curve, and "clearance is longer in accelerating than in decelerating". Figure 2-4 (b) shows that acceleration points (indicated as 'A') and deceleration points ('B') occupy different regions in the speed-clearance plane.

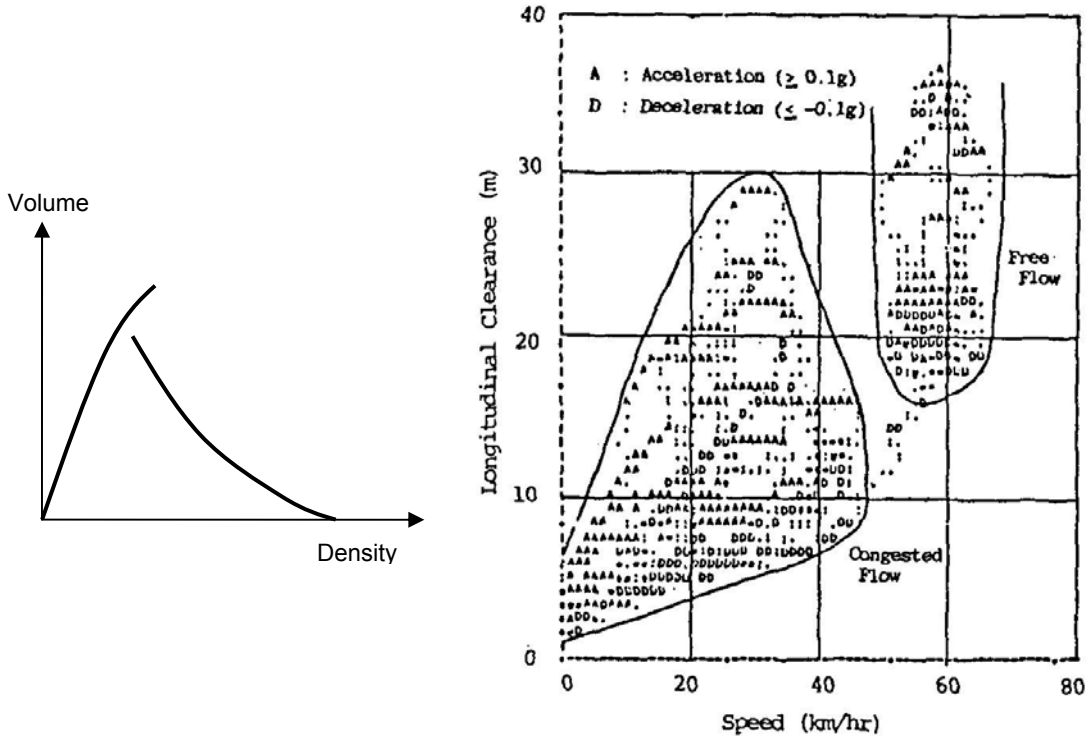

(a) "reverse-λ" shape flow-density relationship (b) Test result, longitudinal clearance

Figure 2-4 Koshi et al. (1983)

Although there have been several sporadic observations on the asymmetric behavior,

theories on asymmetry have not been improved or established since Newell's first work (1965).

Zhang (1999), based on the asymmetry assumption, claimed that "acceleration, deceleration and equilibrium flow should be distinguished in obtaining speed-concentration relationships". He formulated car-following behavior with 3 phases: (1) anticipation dominant, (2) anticipation–relaxation balanced, and (3) relaxation dominant phase. He also formulated car-following models implementing Newell's asymmetry (Zhang, 2005). But this work has not been verified with real data.

Daganzo et al. (1999) gave an explanation on phase transition in highway using simple "Markovian model" following the Newell's theory (1965). They showed how a disturbance in queued traffic grows in congested traffic. Even though this explanation was given as an "incomplete theory" as they said, they showed the potential of the asymmetric theory for explaining traffic phenomena. But, having no empirical data on the evolution of a disturbance, they thought the extension of the asymmetric theory is premature.

Wagner (2004) reported slow-to-start phenomenon claiming that vehicles leave queue with bigger time headway than needed. He also noted that this phenomenon can be explained by Newell's theory (1965), but "by wide fluctuations in congested area, the existence of two branches proposed by Newell might be hidden". Their understanding is limited in that they only noticed on the queue leaving situation not on the general congested one.

Chapter 3 Asymmetric Microscopic Driving Behavior: Basic Theory

As described in the previous chapter, asymmetry in acceleration and deceleration has been observed by many researchers. However, the empirical evidences to date are limited to reveal the whole mechanism of driving behavior. The main obstacle in developing driving behavior theory is the data deficiency at the microscopic level. For real driving behavior is affected by many factors outside of car-following logic (which considers only leader and follower), macroscopic data cannot provide enough information on individual vehicles. Therefore, in this chapter we propose a basic asymmetric driving behavior theory based on a large amount of vehicle trajectory data.

3.1 Driver Behavior: Experimental Evidence

3.1.1 The database

To develop behavioral algorithms for micro-simulation, U.S. DOT (Department Of Transportation) initiated NGSIM (Next Generation SIMulation) program (NGSIM, 2006).

They acquired precise vehicle trajectories dataset at 0.1 sec time interval for four sites including two highways (I-80 in Emeryville, US-101 in LA) and two arterial sites. Highway data of I-80 and US-101 were used for analysis in this research. Figure 3-1 shows the I-80 test site. Located in busy urban area, it has six through lanes including a HOV (High Occupancy Vehicle) lane with total length of 1,650 ft. The I-80 site is located downstream of a merging location of three major freeways: I-80, I-580, and I-880. Also, the freeway section diverges to I-80 and I-580 approximately 2.65 miles downstream. The test section is a Type B weaving section according to the Highway Capacity Manual (HCM2000: Transportation Research Board, 2000) designation. There is a short acceleration lane at the Powell Street on-ramp (147 ft) and a lane drop just downstream of the Ashby Avenue off-ramp. Seven cameras on top of a high rise building acquired the video stream used for tracking vehicle trajectories.

Figure 3-1 NGSIM I-80 site

Figure 3-2 shows US-101 test site which has similar geometry with I-80 site but HOV lane. It has 5 main lanes and one auxiliary lane connecting upstream on-ramp and downstream off-ramp. As shown in the Figure, eight cameras were used for video recording.

From the recorded video stream, they extracted vehicle trajectories using computer vision techniques. At every 0.1 sec, all vehicles in an image frame are detected and tracked automatically. Also, manually editing is applied to improve the result.

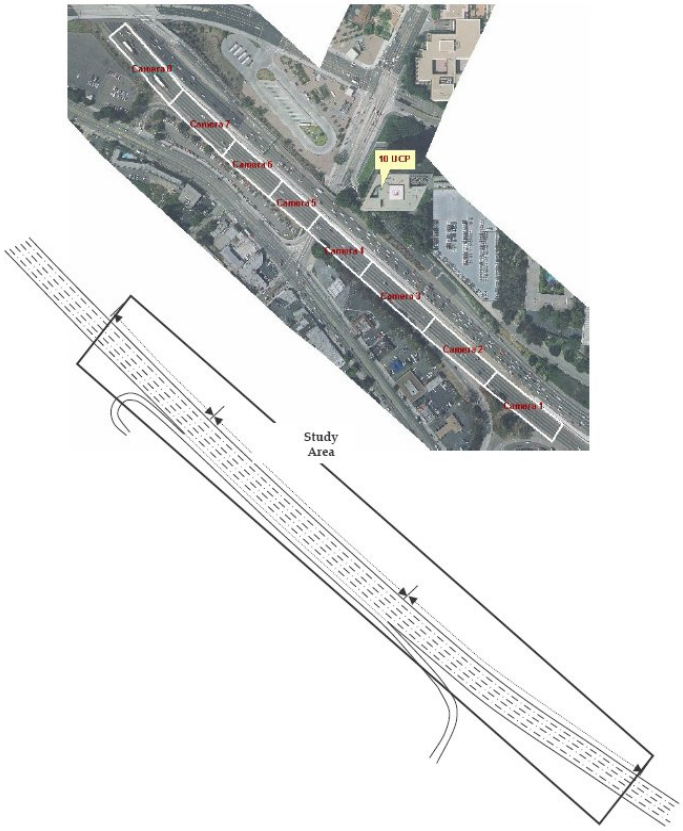

Figure 3-2 NGSIM US-101 site

The compiled NGSIM freeway database consists of vehicle trajectories and aggregate loop detector data for each test site. In the I-80 data set, processed trajectories data include 45 minutes of vehicle trajectories in transition (4:00-4:15 pm) and congestion (5:00-5:30

pm). In the US-101 dataset, processed data include 45 minutes of vehicle trajectories in transition (7:50-8:05 am) and congestion (8:05-8:35 am). The data have been extracted from video recordings using computer vision algorithms. The format is vehicle ID, time, lane and position at 0.1 sec intervals, and derived variables of speed, spacing, and acceleration at the same time intervals are added. A total of 11,779 vehicles were processed.

Figure 3-3 shows a sample of NGSIM trajectories of US-101 site. As the site is a merging section, we can find a lot of stop-and-go waves generated inside the section and propagated from downstream. When traffic passed stop-and-go waves, the speed dropped to 0, and it recovered to 50-60 mph, which is almost free flow, after passing merging location.

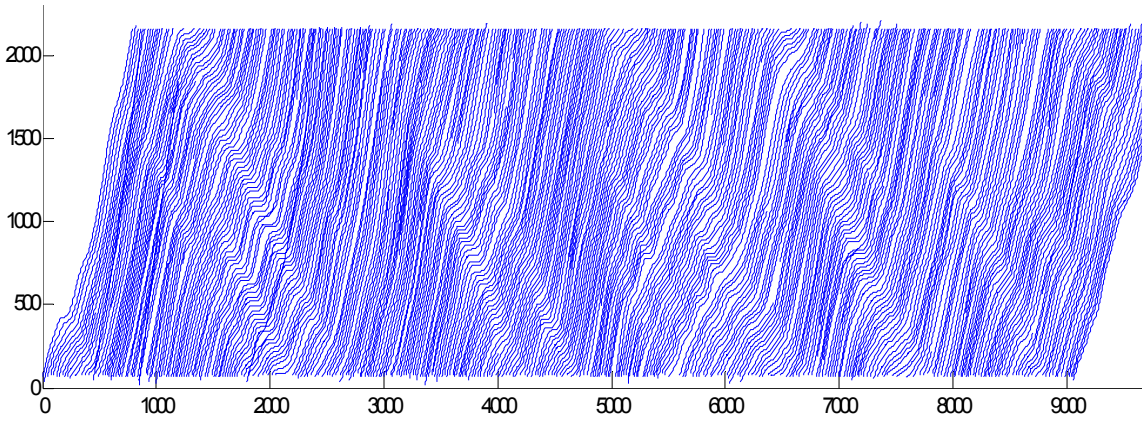

Figure 3-3 NGSIM data example, US 101, Lane 1, 8:20-8:35 am (time x 0.1sec)

3.1.2 Findings: A-curve and D-curve

Real traffic data shows very complicated patterns because of the stochastic and unpredictable nature of the driving behavior. Not only asymmetric behavior but also driver difference, lane changing events, and road geometry affect traffic. Although the actual data

shows very complicated actions, common patterns can be identified by plotting the data in speed-spacing plane for individual vehicles from the total of 11,779 vehicles in the NGSIM database.

In investigating the car-following characteristics, it is very important to filter out lane changing events. So, vehicle trajectories data in the right-most lanes, which are affected strongly by lane changing events, were ruled out when studying traffic phenomena. Also, for other travel lanes, the data were separated before and after lane change event. In case there is a lane change, the spacing has a jump which can be easily identified.

Figure 3-4 shows an example speed-spacing relation for a vehicle from I-80 site data and US-101 site data. The horizontal axis represents spacing which is the distance measured from the front end of the leader vehicle to the front end of the subject vehicle, and the vertical axis represents vehicle speed (i.e. the speed of the subject vehicle at the time when the spacing is measured).

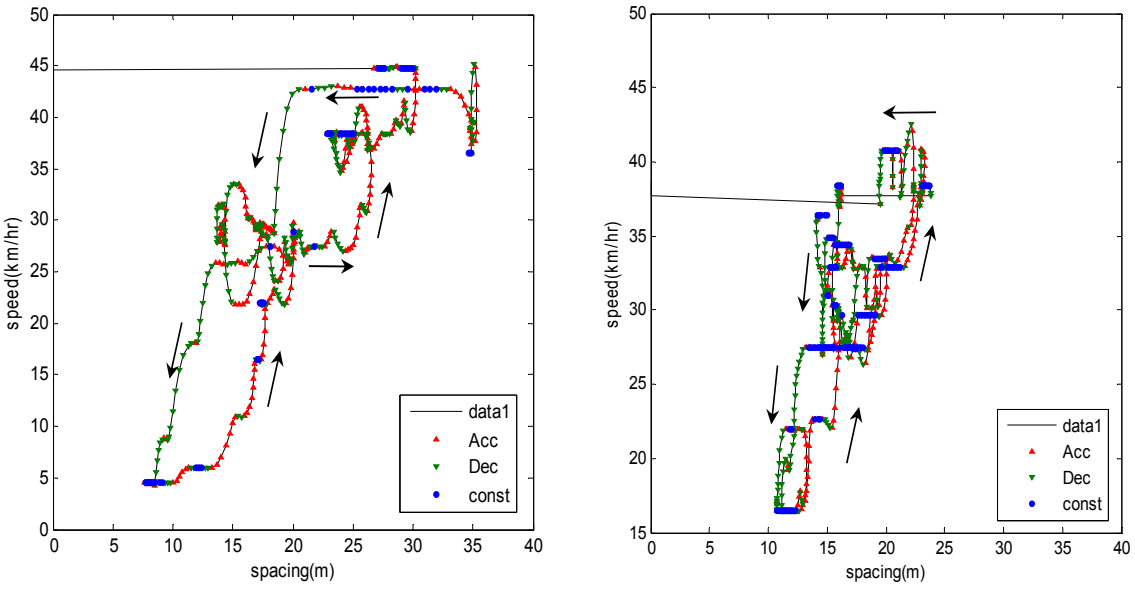

(a) I-80 (b) US-101

Figure 3-4 Example of asymmetric behavior in speed-spacing plane

"Acc" points denote vehicle accelerations greater than 1 ft/sec^2, and "Dec" points denote decelerations with values less than -1 ft/sec^2. "Const" points denote acceleration between -1 and 1 ft/sec^2. When accelerating and decelerating, the drivers follow different path in speed-spacing plane as it was observed by Edie (1965) and Foote (1965). Also between the acceleration and deceleration, the vehicle keeps constant speed as illustrated as "const" in the figure.

Figure 3-5 shows another example of speed-spacing plot for a vehicle from I-80 test site. In this example, we can clearly identify two separate groups of data forming virtual lines denoted as 'A-curve' and 'D-curve'. We follow the naming of Newell's two-curves (1965). The acceleration curve (A-curve) can be separated from the deceleration curve (D-curve), and is lower than the D-curve in speed-spacing plane. The A-curve and D-curve define a 2-dimensional region in which the traffic is in equilibrium. A-curve is the boundary curve from acceleration side, and D-curve is the one from deceleration side. As boundaries of the equilibrium region, acceleration or deceleration actions are outside of the A/D curve. So, connecting the points where acceleration actions stop, we can find A-curve as shown in Figure 3-5. In the same way, D-curve can be found by connecting the stopping points of deceleration actions. A-curve and D-curve are used as a desired spacing which is a target in acceleration and deceleration.

The dotted lines called acceleration and deceleration action point lines can be found by connecting starting points of acceleration or deceleration actions. The location of these curves can vary according to speed difference between leader and the follower. The constant speed state can be found in every cases of Figure 3-4 and 3-5. This time period varies from 1-5 sec according to traffic situation such as speed difference and gap

difference. This time of coasting implies that the equilibrium lies on a 2-d region and the constant speed period is the time needed to traverse this region. Sometimes it is observed that the direction of coasting (towards A-curve or D-curve) can be changed. This can happen when a leader vehicle changes its sign of acceleration.

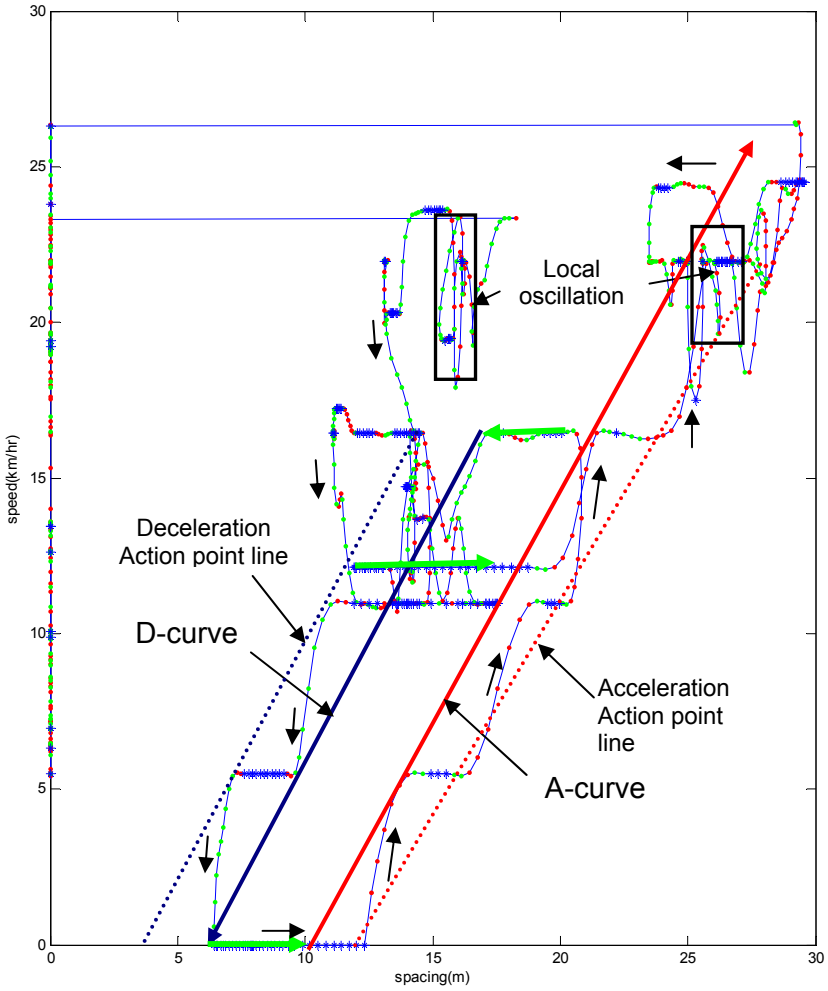

Figure 3-5 Driving behaviors in speed-spacing plot, I-80.

Also, we can find local oscillation points. In Figure 3-5 the speed variation of the oscillation is less than 5 km/hr and the spacing variation is less than 3m. These points are

also found in Figure 3-4 though it has bigger speed variation. The locations of local oscillation are near on the A/D-curve in Figure 3-5 and inside the two curves in Figure 3-4.

In summary, we can observe the following phenomena from the speed-spacing plots:

(1) Separation of accelerations and decelerations (A-curve and D-curve).

(2) Constant speed state connecting accelerations and decelerations.

(3) Local oscillation points lying between accelerations and decelerations.

3.2 Possible Causes of Asymmetric Behavior

At this time we also have to think about the origin of the asymmetry. Newell (1965) postulated that "If some car accelerates, the driver behind it will intentionally allow a certain excess headway to develop." And, the driver will "wait and see" to check if the pattern persists. It looks so natural that human behaviors are asymmetrical because complete symmetry cannot be attained when there are two different kinds of actions available. Acceleration and deceleration are two separated situation in which driver's psychology is different. Besides the above, we can consider other factors affecting the asymmetry in acceleration and deceleration.

3.2.1 Sampling and vehicle performance limit

It has been thought that drivers' acceleration can be regarded as a continuous action in time space. In Newell's, the vehicle moves along A/D-curve continuously, but in the examples shown in the previous section, we cannot find smooth curves during the acceleration or deceleration. Instead, stepwise acceleration and deceleration can be found, and the concept of driver's 'discrete sampling' of traffic situation, and 'discrete action'

seems to fit more.[1] Drivers sample the driving situation in a discrete manner not continuously, for example, when a driver follows a leader vehicle, he/she will check spacings and speeds every 1 second. This procedure will result in the stepwise acceleration behavior shown in the Figure 3-6. Same patterns can be found in Figure 3-3, Figure 3-4 and Figure 3-5. In Figure 3-6, each time period of acceleration form point '3' to '4' is around 0.6 sec, and then there are pauses of acceleration for 0.3~0.5 sec before the next action.

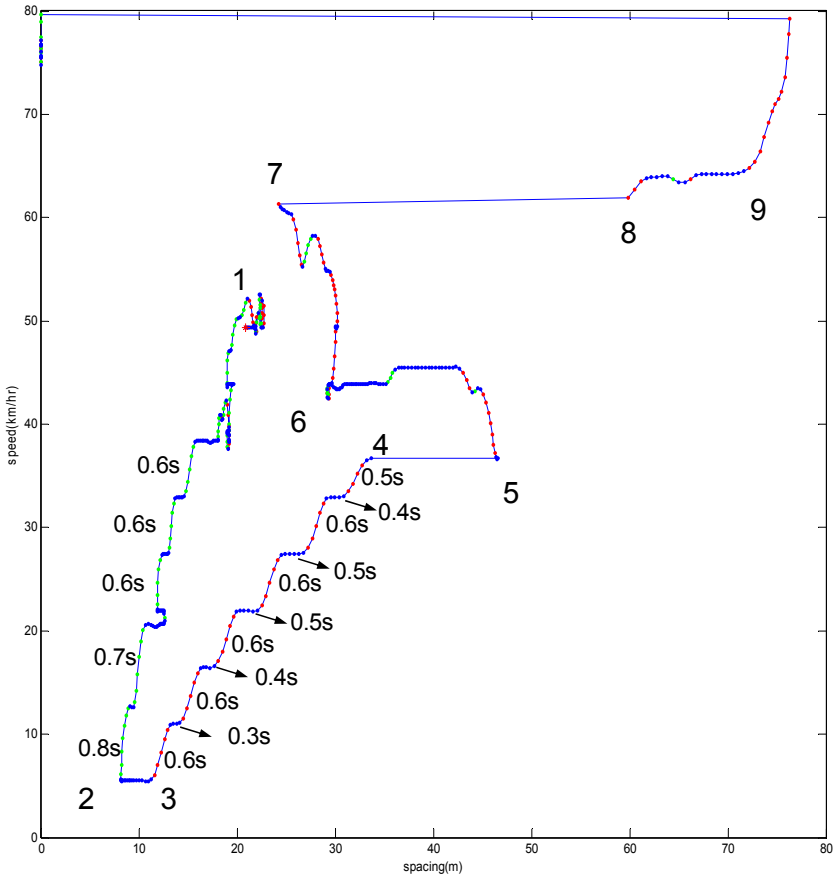

Figure 3-6 Sampling behavior, speed spacing relation for a vehicle, US-101

[1] See Daganzo (1999) pp. 142

So, we can say that the driver in Figure 3-6 is sampling traffic situation every 0.9~1.1 sec, acting for about 0.6 sec and pausing for about 0.3~0.5 sec to decide on the next action. This tendency also can be found in deceleration case from point '1' to '2'. In case of moving after point '9', the acceleration period is extended because the vehicle is speeding up to free flow, which does not need to check the front vehicle's speed and gap frequently.

Besides the sampling behavior, there also exists a performance difference between vehicles and their preferred acceleration rates. If a vehicle cannot catch up with the speed and spacing of the lead vehicle, it causes a lag in acceleration or deceleration. In case the acceleration period lasts long, the lag will form a hysteresis loop even with the one-curve situation as shown in Figure 3-7 (a).

When a vehicle starts from point '1', if the spacing gets larger, it starts acceleration at point '2'. When there is no performance limit or the acceleration capability is enough, the vehicle will move to point '3' which is close to the preferred equilibrium states. When sampling is applied during the sampling time period used for situation checking and decision, the traffic states will deviates from the equilibrium curve as in case 'A', but finally after having acceleration actions it will move back to equilibrium location '9' on the curve.

When performance is limited or the preferred acceleration rate is less than the one of the lead vehicle, the gap between the equilibrium curves gets bigger as in case 'B'. The difference between one curve and two-curve theory lies in the starting point and end the point location in speed spacing diagram. In two–curve theory, because the equilibrium states exist as a plane not a curve, the action starting and ending point '1', and '9' are shifted to right direction to larger spacing as in (b).

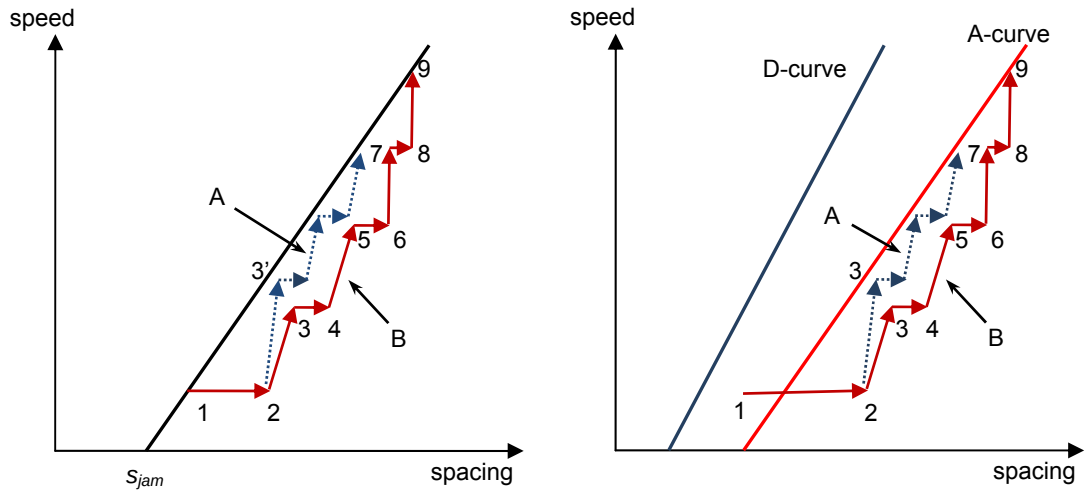

(a) One curve case (b) Two-curve case

Figure 3-7 Sampling with performance limit

3.2.2 Driver's aggressiveness

Driver's aggressiveness can be defined using three variables: jam spacing (s_{jam}), wave travel time (t_w) and free flow speed (v_f) in linear model as illustrated in Figure 3-8. Aggressive drivers keep short gaps and have short reaction time resulting in short wave travel time, and high free flow speed. It has been usually assumed that a driver's aggressiveness does not change over time during a trip in simulation. But, in real driving situations they can also change.

In asymmetric theory's view, drivers are usually relaxed in acceleration situation, in other words, less aggressive. Drivers have larger gap and bigger wave travel time. While in deceleration situation, drivers are more aggressive (i.e., keeping very short gap), and very sensitive and ready to react promptly (i.e., have less wave travel time).

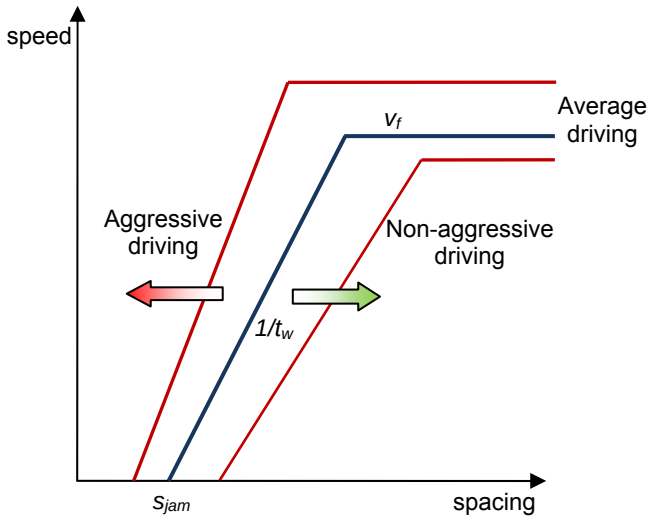

Figure 3-8 Aggressiveness in driving

3.3 Proposed Theory: Traffic Phases

From the findings described in the previous section, we can define traffic phases based on asymmetry in acceleration and deceleration. Each driver is supposed to have his/her own A-curve and D-curve. Figure 3-9 illustrates an individual driver's A/D curve and traffic phases. Even though we illustrate the A-curve and D-curve as linear, it has to be noted that the curves are not necessarily linear. The shape of the curves will be discussed later in Chapter 7.

An individual vehicle's traffic state can be classified into 5 phases according to speed and movement of the vehicle: Free flow, acceleration, deceleration, stationary and coasting. Figure 3-9 (a) depicts these five phases in speed-spacing plane, and Figure 3-9 (b) in flow-density plane. Free flow is a traffic state in which a small disturbance does not affect upstream traffic. In other words, if a vehicle is in free flow phase, a small speed change or spacing change from leader vehicle does not trigger a deceleration action of the subject

vehicle. In free flow, drivers run at their desired speed which is usually a maximum speed. Acceleration phase is a state in which a vehicle is speeding up to catch up with the speed of the lead vehicle or reduce spacing. It includes the time period for reaction before the actual action starts. So, it can be regarded to start from the point where the vehicle departs its A-curve. In deceleration phase a vehicle is braking to reduce its speed or to increase spacing from the lead vehicle. In stationary phase, vehicles keep constant both their speed and spacing.

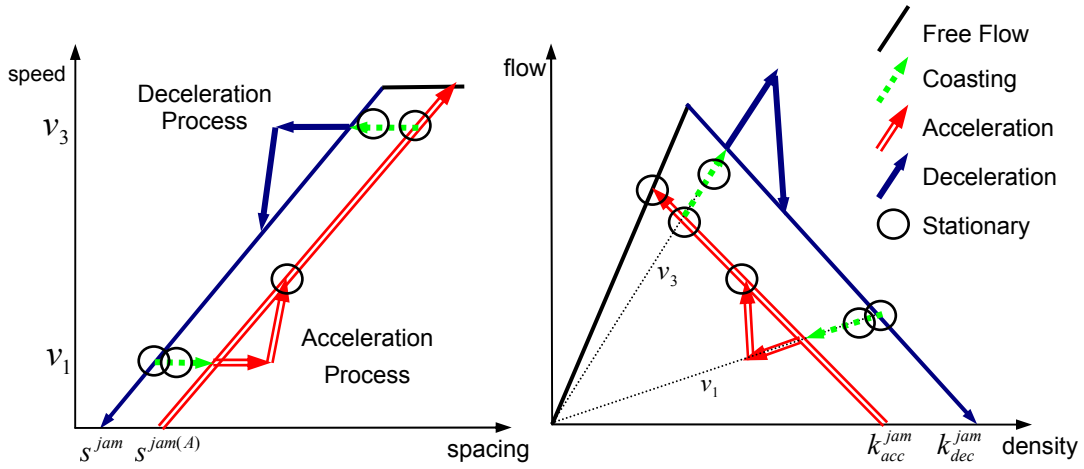

(a) Phases in speed-spacing plane (b) Phases in flow-density plane

Figure 3-9 Traffic phases

Coasting is defined as a phase in which a vehicle keeps its speed but spacing is being reduced or enlarged by the lead vehicle's deceleration or acceleration between A/D curve. During coasting phase, a vehicle will not do any action as long as it is between the two curves. Reaching A or D-curve, it will start acceleration or deceleration phase. Coasting is actually a transition phase connecting deceleration and acceleration. The existence of coasting phase can be thought as an evidence of two-curve because the longer coasting

period implies the bigger separation between the A- and the D-curves. Also note that the minor acceleration and deceleration inside the A/D curve is regarded as part of the stationary not acceleration or deceleration phase. Detailed explanations on each phase are given below.

3.3.1 Acceleration and deceleration phase

Consider a situation as shown in Figure 3-10. It shows both acceleration and deceleration processes. Assuming instant acceleration, we can compare the trajectories of the new theory (solid lines) with the ones (dotted lines) from Newell's simplified car-following theory (2002) which conforms to LWR theory.

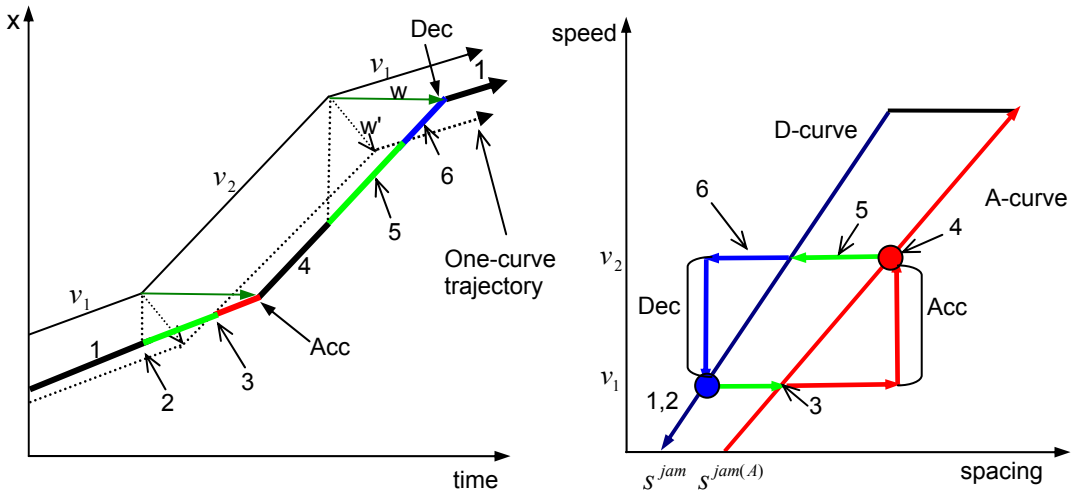

(a) Expected time-space plot of example (b) Speed-spacing relation of example

Figure 3-10 Transition between traffic phases

If a vehicle starts from state '1' on D-curve with short spacing and the lead vehicle accelerates, the spacing will be enlarged until the vehicle reaches to point '3' on A-curve.

From this point, the following vehicle will change driving mode to acceleration. After securing sufficient spacing for the new speed, it will speed up and reach state '4'. The vehicle can stay on state '4' until the lead vehicle changes its speed, so state '4' can be an equilibrium point on A-curve. If the lead vehicle starts braking, the subject vehicle will not start deceleration until it reaches D-curve. Passing D-curve, it will start deceleration and find a new equilibrium at point '1'. As shown in Figure 3-10 (a), in phase transition, the wave speed w is slower than the one in LWR theory denoted as w'.

3.3.2 Stationary and coasting phase

In microscopic view, stationary phase is a traffic state in which the speed and spacing between two adjacent vehicles are constant. But, in traffic situation it is almost impossible for these two values to be kept constant for long time because human perception and reaction are not perfect. So, we need a relaxed definition for stationary phase. Near-stationary flow can be defined in speed-spacing plane when the following conditions are satisfied:

$$\left|\frac{ds_n}{dt}\right| \le TH_s\,,\ \left|\frac{dv_n}{dt}\right| \le TH_v$$

Where, TH_s and TH_v is threshold value for spacing and speed respectively.

The speed thresholds in the previous examples are within 3 km/h ~ 5km/h, and spacing thresholds are 5 m, which looks reasonable. This threshold values can be easily determined by obtaining the distributions of the variations from real trajectories data. Stationary sets of points can exist anywhere between A-curve and D-curve. Without significant change of leader vehicle's speed, the follower tries to keep current speed and spacing by adjusting

speed resulting in oscillatory behavior in speed and spacing.

In case of significant change in speed and spacing, a vehicle can coast keeping same speed and delaying an action decision until it reaches A or D-curve. According to the leader vehicle's speed change, we can observe oscillatory behaviors with same speed between the two curves. This decision-delaying region is similar to the concept of perception range in psycho-physical model (Wiedemann and Leutzbach, 1986) and the clouded area of synchronized flow in Kerner's three-phase theory (Kerner, 2004). In the proposed asymmetric theory, the equilibrium is defined as a region bounded by two curves while psycho-physical model has one latent equilibrium curve with wide scattering region from the human perception limit. Kerner's synchronized flow also has a region of equilibrium, enveloped by two boundary curves (safety curve and synchronization curve), but the behaviors inside the regions are regarded as random events and not well explained, while the proposed theory has focused on the behaviors inside the wide scattering region. Note that in Kerner's theory synchronization curve is used for larger spacing traffic, but in the proposed one the larger spacing traffic is caused by acceleration.

Figure 3-11 is an example showing traffic phases. 'A', 'B' denotes acceleration and deceleration phase respectively, 'S' and 'C', stationary and coasting phase. Upward triangles represent acceleration points, downward ones deceleration points, and circles indicates constant speed points. The two solid lines represent A/D curve respectively. The right curve is A-curve and the left one for D-curve. Also note that to determine A/D curve, we need longer time periods data of driving to have long-run average equilibrium region for the human behavior can fluctuate with time and short term situations.

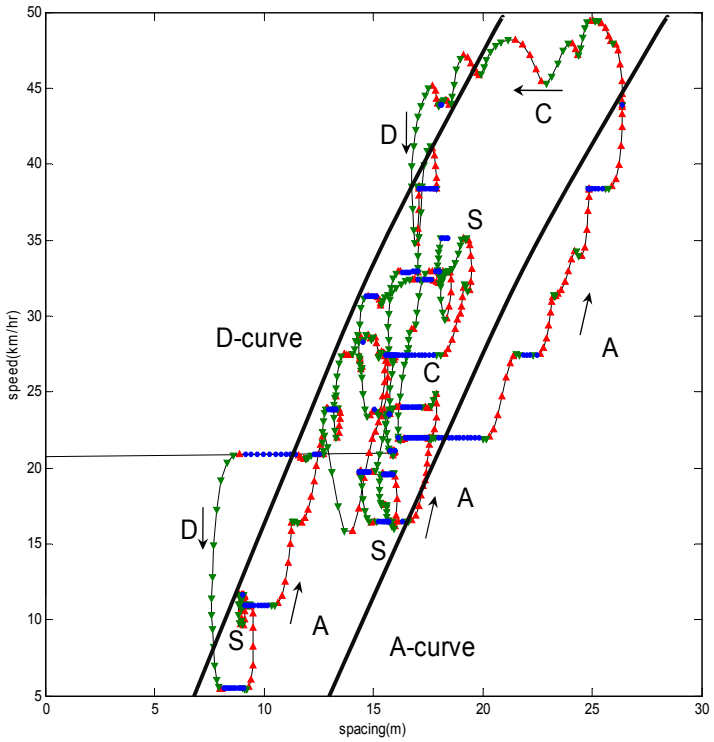

Figure 3-11 Traffic phases in NGSIM data, US-101

3.4 Shock Waves

3.4.1 Reaction time vs. Wave travel time

It has been observed that the human reaction time to front stimulus is different from the actual response time which is measured from front speed change to the follower's speed change on the road. Here, wave travel time will be used instead of response time. Reaction time includes perception and decision time which has minimum value around 0.5 sec. Kim and Zhang (2004) called this reaction time as 'biological reaction time', and wave travel time as actual reaction time. Figure 3-12 shows measured reaction time in

car-following for deceleration situation (Trigs, and Harris, 1982).[2] The time gaps between the lead vehicle's braking signal and follower's signal were measured. It shows a distribution which ranges from 0.5 sec~1.6 sec. Most of them (80%) are within 0.6 sec~1.3 sec. This distribution shows good match with real human reaction time.

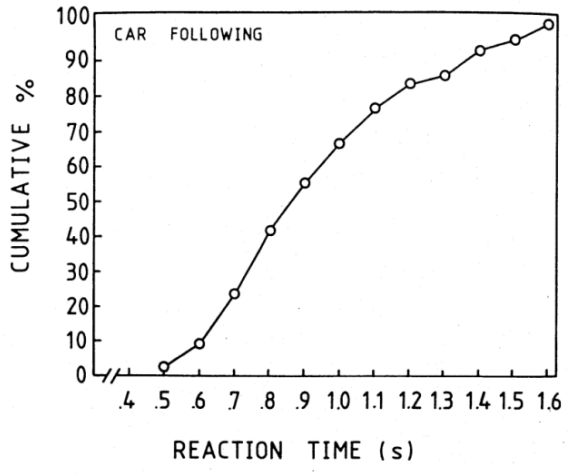

Figure 3-12 Reaction time in Car-following (Trigs, and Harris, 1982)

In contrast to the previous measurement, Figure 3-14 shows wave travel time distribution ranging from 0~5 sec. The distributions are extracted from both acceleration cases and deceleration cases in NGSIM trajectories data by measuring the time gap between speed changes of lead vehicle and following vehicle as described in Yeo and Skabardonis (2008) (Figure 3-13). The wave travel time τ can be found by measuring the time difference between two vehicles' action points (acceleration or deceleration). If a lead vehicle started decelerating at time t_1 and the subject vehicle started at time t_2, the wave travel time τ is t_2 - t_1, if all of the following conditions are satisfied:

[2] Even though this experiment is close to measuring wave travel time by definition, but the experiments was done for limited situation of braking, the result obtained measurents closer to reaction time.

- The subject vehicle's speed must be less than free flow speed
- Both vehicles must travel at a constant speed before the action
- Both vehicles must be traveling at the same speed before the leader vehicle's action

Figure 3-14 shows the measured distribution of the wave travel times and the fit of the lognormal distribution to the data on each site.

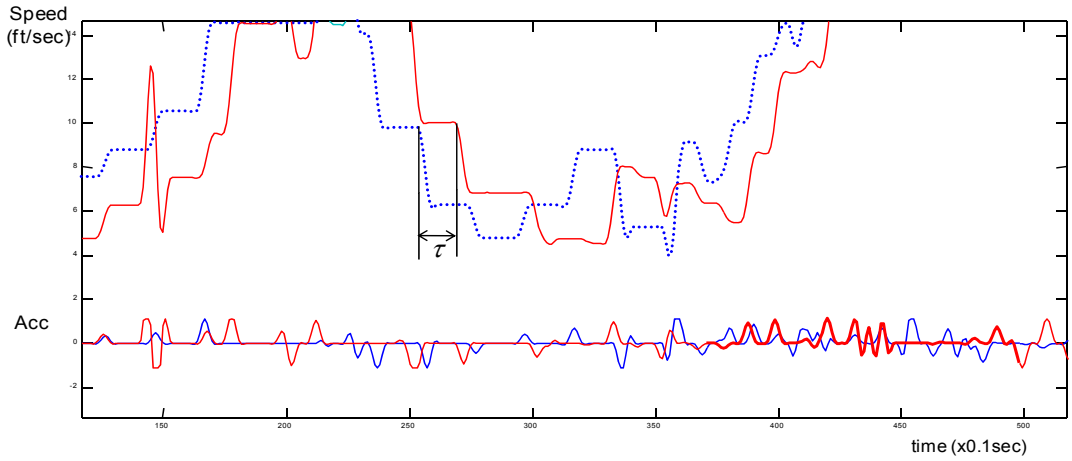

Figure 3-13 Measurement of wave travel time (τ)

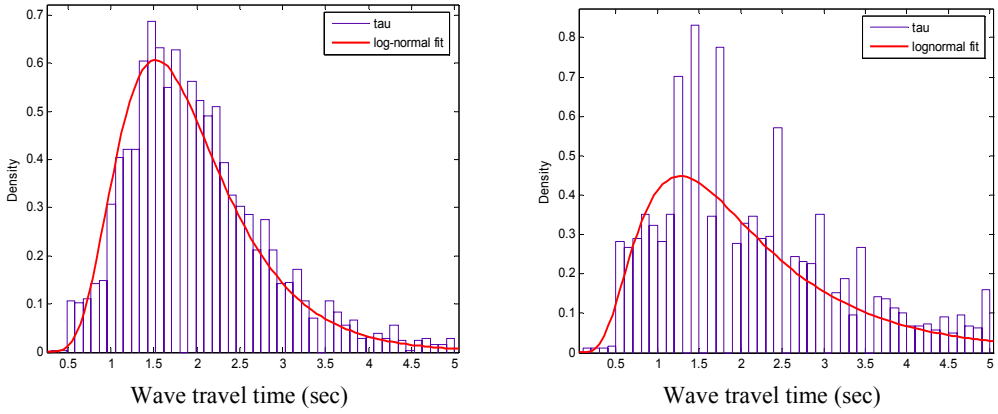

(a) US101 (b) I80

Figure 3-14 Wave travel time distribution and lognormal fitting

From the proposed theory perspective, we can find the reason of difference in reaction time and wave travel time. As in Figure 3-15 case (B), the wave travel time is coasting time + reaction time. The longer the coasting period, the longer is the response time. Therefore, because of the coasting period, reaction time distributions cannot be easily measured from real traffic. Reaction time can be obtained with enhanced condition that the spacing before deceleration must be outside of the A/D curve boundaries as shown as case (A) in Figure 3-15.

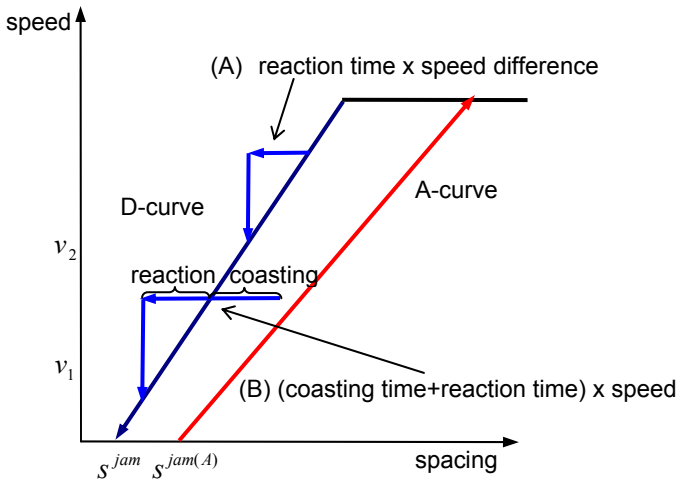

Figure 3-15 Reaction time and response time

3.4.2 Shock wave speed

As shown in the previous section, the wave travel time of following vehicle depends on the traffic state defined by speed and spacing. Therefore, the speed of shock wave propagation can be obtained as follows (Newell, 1965).

Assuming two states A(s_1, v_1) and B(s_2, v_2) which are on different curve in speed-spacing plane. Shock wave propagation time to change from state A to B is

$$t_w = \frac{(s_2 - s_1)}{(v_2 - v_1)} \tag{3-1}$$

The wave travel distance is

$$d = (v_2 t_w - s_2) \tag{3-2}$$

Therefore, wave speed w is

$$w = \frac{(v_2 t_w - s_2)}{t_w} = v_2 - s_2 \frac{v_2 - v_1}{s_2 - s_1} \tag{3-3}$$

$$w = v_2 - s_2 \frac{v_2 - v_1}{s_2 - s_1} \tag{3-4}$$

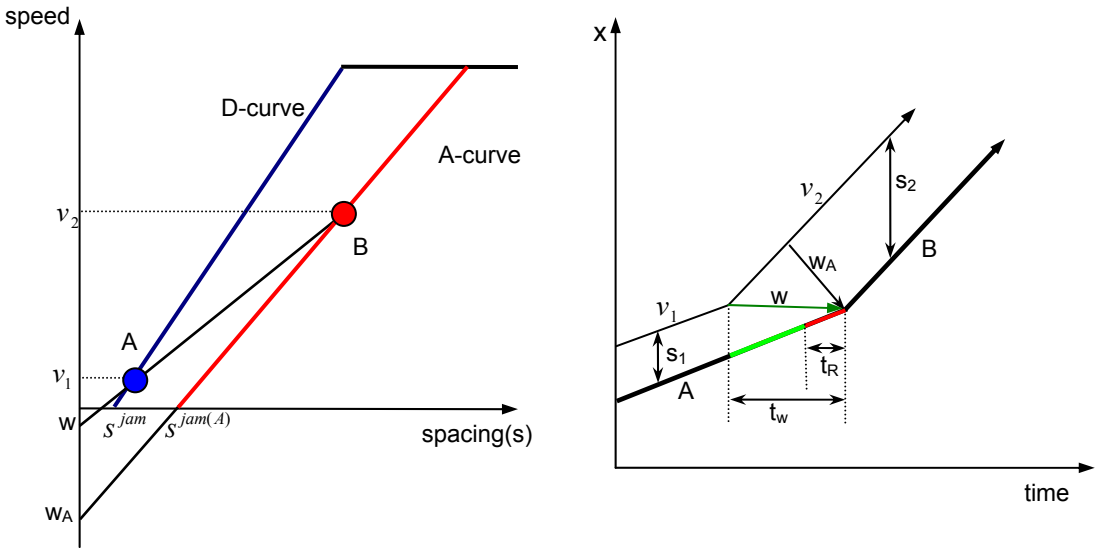

Figure 3-16 Wave speed in asymmetry

As shown, the shock wave speed between two points is the y-intercept of the line connecting two points. If the transition is made between deceleration and acceleration, the shock wave speed is slower than other cases when the transitions occur on the same curve. This time delay of shock wave between different curves is due to coasting phase. As Newell (1965) noticed, the different wave speeds are one of the reasons of instability.

Chapter 4 Theory Extension: Human Driving Behavior

In the previous Chapter, we described a microscopic driver behavior theory based on extensive analysis of individual vehicle trajectories. However, driver behavior is a very complex process, and it cannot be fully explained with the proposed theory. Examples include different responses to same driving situations, maneuvering errors, and differences in following behavior.

A typical example of driving behavior which cannot be explained with the theory described in Chapter 3 is the over-reaction phenomenon. When a leader vehicle changes speed, the following vehicles' speed changes are sometimes greater than the leader vehicle. This phenomenon was first observed by Herman and Rothery (1965). They measured speeds of 11 vehicles in a platoon. The top part of Figure 4-1 shows the speed of the leader vehicle, the middle part shows the speed of the 6th vehicle and the bottom part shows the speed of the last vehicle in the platoon. The difference in speed change was amplified as it propagated upstream in the platoon.

In this Chapter, we describe the extension of the proposed theory to address two

commonly observed patterns of driver behavior, namely maneuvering errors and anticipation, based on further analysis of empirical data.

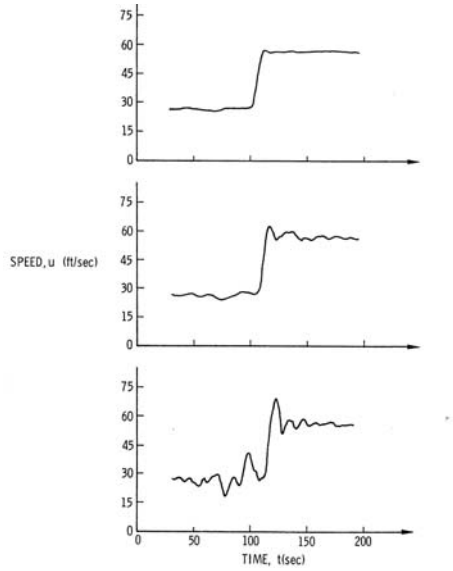

Figure 4-1 Over-reaction observation in Herman and Rothery (1965)

4.1 Maneuvering Error

Drivers are not perfect in adjusting their speeds, because of perception, estimation and action errors. Perception errors include measurement errors for distance or speed of the vehicle in front. Estimation means the process of assessing the response to the perceived actions of other vehicles, i.e. when a leader vehicle starts braking the follower has to determine the amount of deceleration. Action errors refer to the error in implementing the derived responses by controlling mechanical components of vehicle.

Regardless of their causes, errors appear as under-reaction or over-reaction. In under-reaction case, the amount of action (acceleration or deceleration) following the leader vehicle's speed change is less than the required value while in over-reaction the amount of action is greater. Figure 4-2 (a) shows examples of maneuvering error in

deceleration case. Under-reaction or over-reaction is followed by additional speed adjustment which forms a secondary wave, i.e. a wave can split during its propagation to upstream. In both cases, the minimum speed of the following vehicle is lower than the one of the lead vehicle. This can amplify the impact of a disturbance when following vehicles are near D-curve location while it can dissipate when the following vehicles are near A-curve which has enough spacing not to be disturbed by a small disturbance.

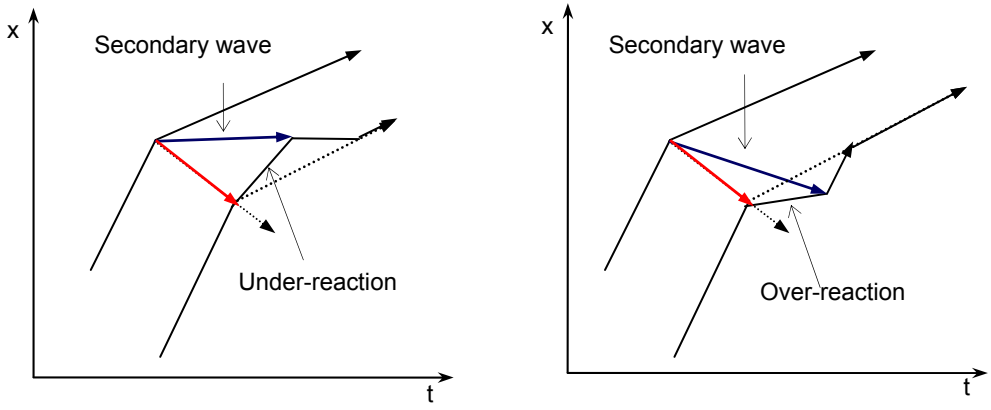

(a) Deceleration case

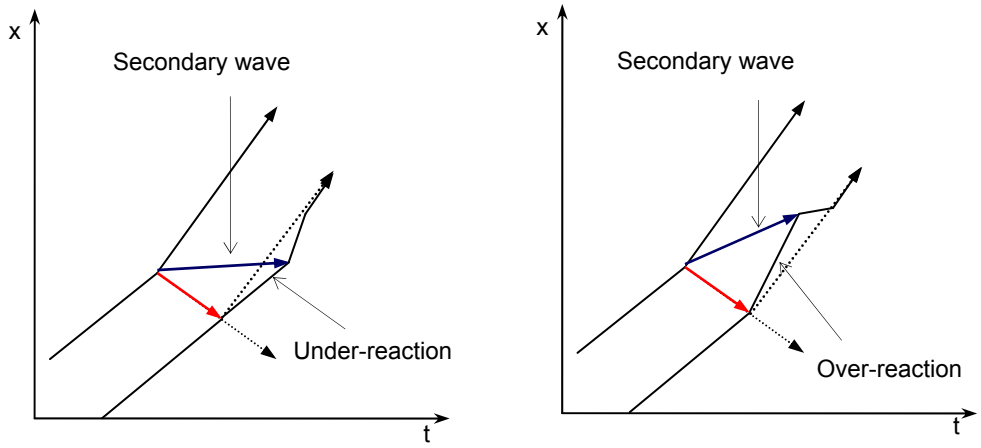

(b) Acceleration case

Figure 4-2 Wave split and anticipation effect.

Figure 4-3 shows the effect of the under-reaction. The dotted line represents expected trajectories without under-reaction. A vehicle under-reacted for the front stopping wave, i.e. a late response was made. Then, the driver had to brake so that its speed is low enough to make its traffic state to quickly move back to safe region.

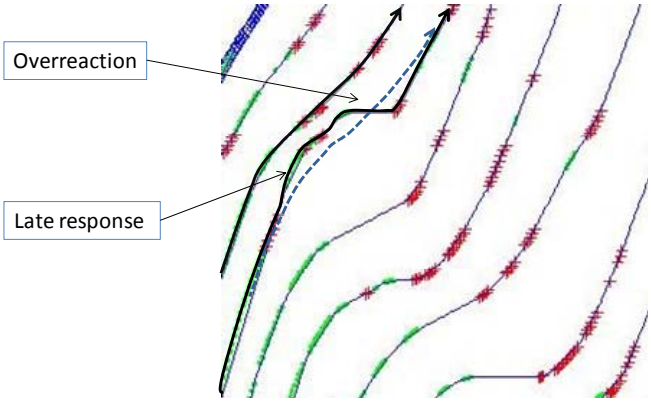

Figure 4-3 Maneuvering error by under-reaction

Figure 4-4 shows how the over-reaction propagates through a platoon. It shows 3 vehicles with decreasing minimum speed. For the first vehicle the minimum speed was 20 kph for short time period. But as it propagated to upstream vehicles, the minimum speed dropped to 18 kph, and finally 16 kph for the 3rd vehicle. Also the time period of this minimum speed increased.

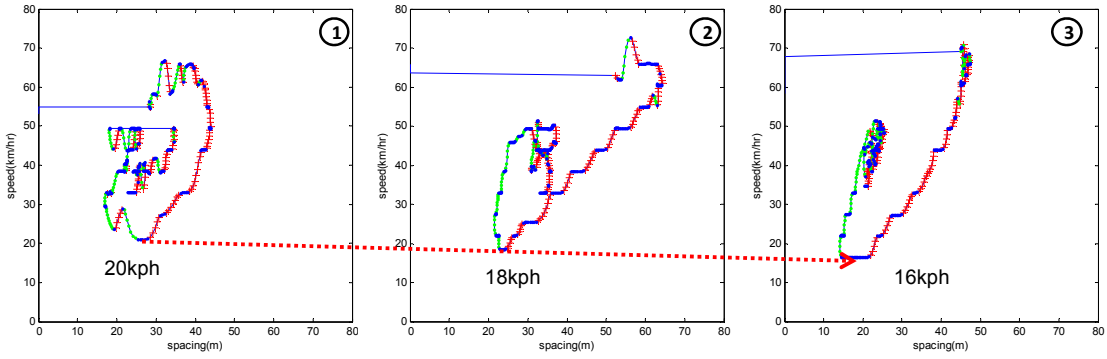

Figure 4-4 Minimum speed drop in platoon vehicles in deceleration case.

4.2 Anticipation

The "anticipation effect" is related to the time of action on the possible change in future traffic. In most car-following models, it is assumed that drivers follow only one vehicle, but in the real world, drivers use information from several vehicles downstream and even from adjacent lanes. Furthermore, if a certain traffic phenomenon is recurrent on a certain location, drivers might also be familiar with it, and adjust their behavior accordingly. If drivers can predict the state of downstream traffic, they can avoid sudden change in speed and keep comfortable driving spacing. If faster speed in downstream traffic is expected, a driver can start accelerating earlier, and if deceleration is anticipated, a driver can start braking in advance, or delay acceleration. Thus, the anticipation effect can cause both shorter reaction times physically infeasible and longer reaction times than needed. Some researchers (Wagner, 1998; Hoogendoorn et al., 2007) proposed car-following models including several vehicles, and others (Treiber et al., 2005) introduced anticipation effects in car-following model formulation.

Figure 4-5 shows acceleration anticipation case. τ_a is the time of action after leader vehicle's action. τ_d is the anticipated duration time of acceleration. Assuming that the current traffic state is '1' in (b), a driver can determine action depending on the anticipated time, τ_d. In normal case without anticipation, i.e. τ_d=0, the vehicle will follow path '2'. If $\tau_d > 0$, it will follow path '3'. In case of bottleneck discharge when free flow is expected in downstream location, an aggressive driver can adopt path '4' which is passing between the two curves. Figure 4-6 depicts the deceleration case. The mechanism in deceleration case is same with acceleration case.

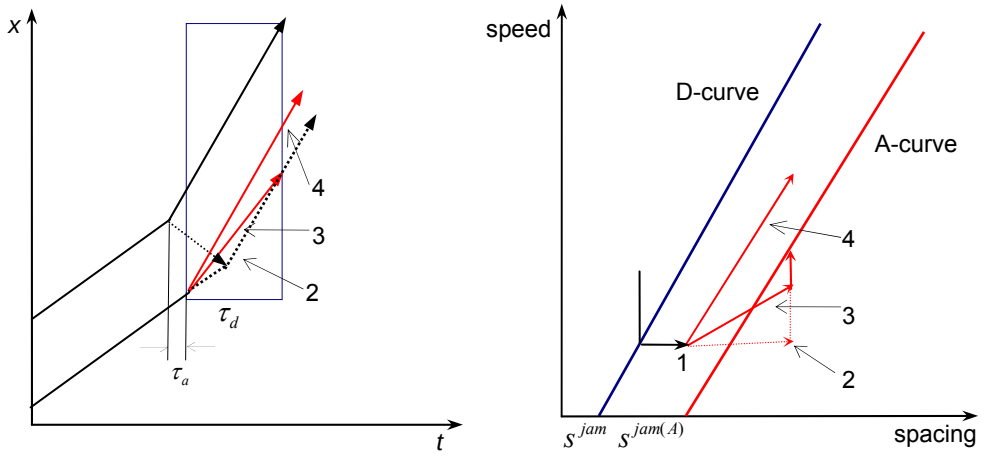

(a) Vehicle trajectories in time-space. (b) Anticipation in speed- spacing.

Figure 4-5 Anticipation effect in acceleration.

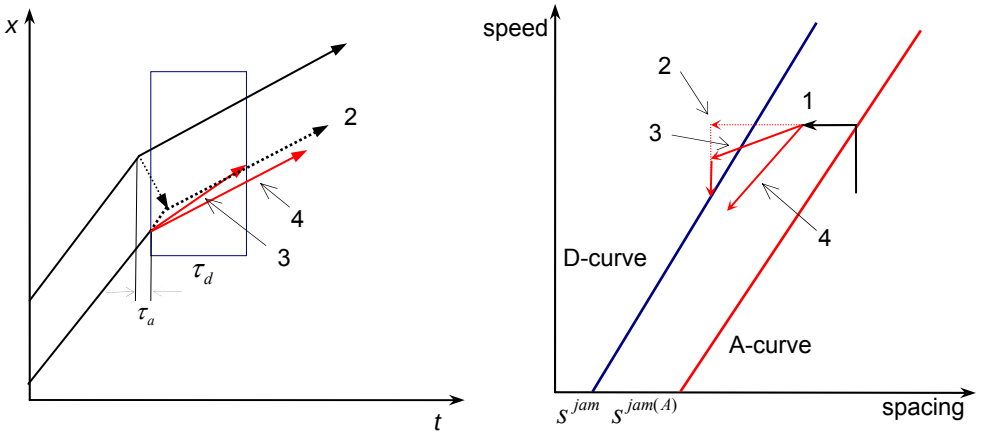

(a) Vehicle trajectories in time-space. (b) Anticipation in speed- spacing.

Figure 4-6 Anticipation effect in deceleration.

Figure 4-7 shows the trajectories of several vehicles experiencing slow-down. Circles (•) represent decelerating points, and cross (+) symbols represent accelerating points. The regions without circles or cross symbols in the trajectories belong to constant speed points. Arrows represent the propagated waves. As shown in the Figure, the first wave of

deceleration is very fast comparing with the other waves. The vehicle '1' starts decelerating almost at the same time with the leader vehicle. This faster action is physically impossible and cannot be explained without driver's perception of downstream traffic. It can be also found that this anticipation effect is not applied to the vehicle '2' and '3' when they are decelerating. The choice of anticipation is probabilistic in nature according to driver's characteristics such as vehicle class and aggressiveness.

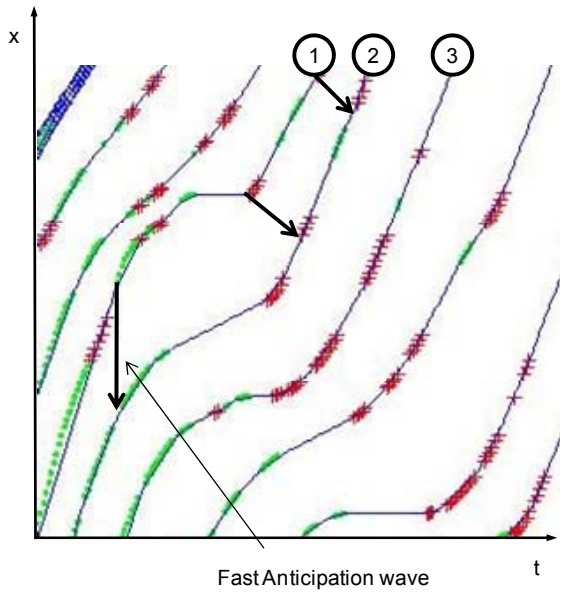

Figure 4-7 Anticipation wave in time space. US-101 site example.

The anticipation effect is shown in the speed-spacing diagram (Figure 4-8). When a vehicle anticipates a stop-and-go traffic, i.e. a deceleration wave followed by acceleration wave, a driver decelerates more than needed, and starts acceleration earlier before it reaches the A-curve. This case is illustrated as case 'A' in the Figure. As a result, its coasting phase between D- and A-curve is reduced. Case 'B' shows the earlier acceleration by anticipation, and as a result of the too early acceleration it has additional coasting period before it start accelerating again. Note that in the examples in Figure 3-4 and Figure 3-5,

they do not show this earlier starting action behavior, and instead, they show coasting phase. Therefore, in anticipation case, the action points of acceleration and deceleration can be inside of the equilibrium region. And the action points' lines cannot be determined as fixed curves, and has to be derived considering anticipation.

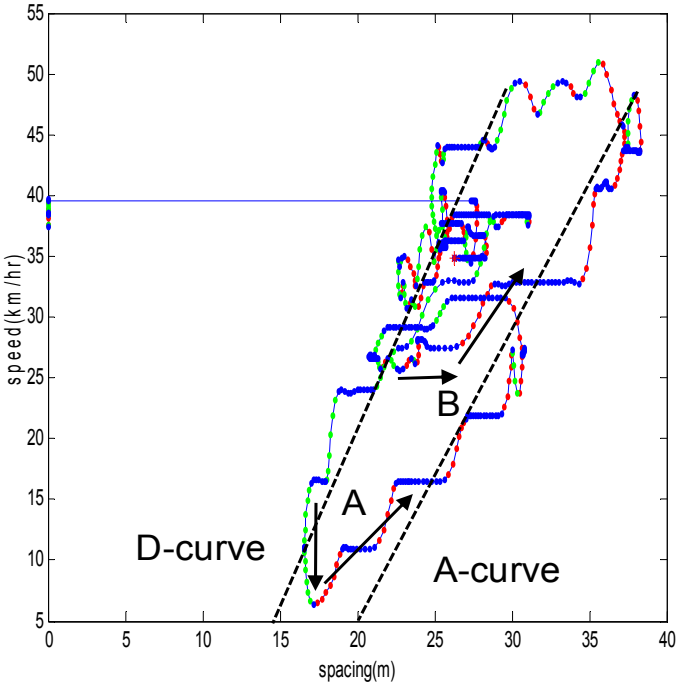

Figure 4-8 Anticipation in speed-spacing relation. US-101 site example.

Chapter 5 Theory Application I: Hysteresis, Stability, Capacity Drop and Relaxation after Lane Change.

In Chapter 3 and Chapter 4, we described a microscopic asymmetric traffic theory and its extensions. The proposed theory is applied to explain several traffic phenomena in congested traffic. This Chapter describes the application of the theory on traffic hysteresis, traffic stability, capacity drop and relaxation after lane change event.

5.1 Traffic Hysteresis

Hysteresis, originated from Greek words, means "Lagging behind". In traffic engineering, traffic hysteresis indicates the phenomenon of retardation in speed recovery. The proposed asymmetric theory is a natural explanation on the hysteresis phenomenon. The separation between the A-curve and D-curve forms hysteresis loops as observed first by Edie (1965). In the proposed theory, a pair of acceleration and deceleration actions can form a hysteresis loop. This pair-wise action (deceleration-acceleration or

acceleration-deceleration) can be easily found when traffic meets stop-and-go wave which occurs frequently in congested traffic.

Treiterer and Myers (1974) used vehicle trajectory data from aerial photographs (Figure 5-1), and developed the flow-density diagram shown in Figure 5-2 (a). Traffic states' change forms a double loop of two different direction cycles denoted as 'A' and 'B'.

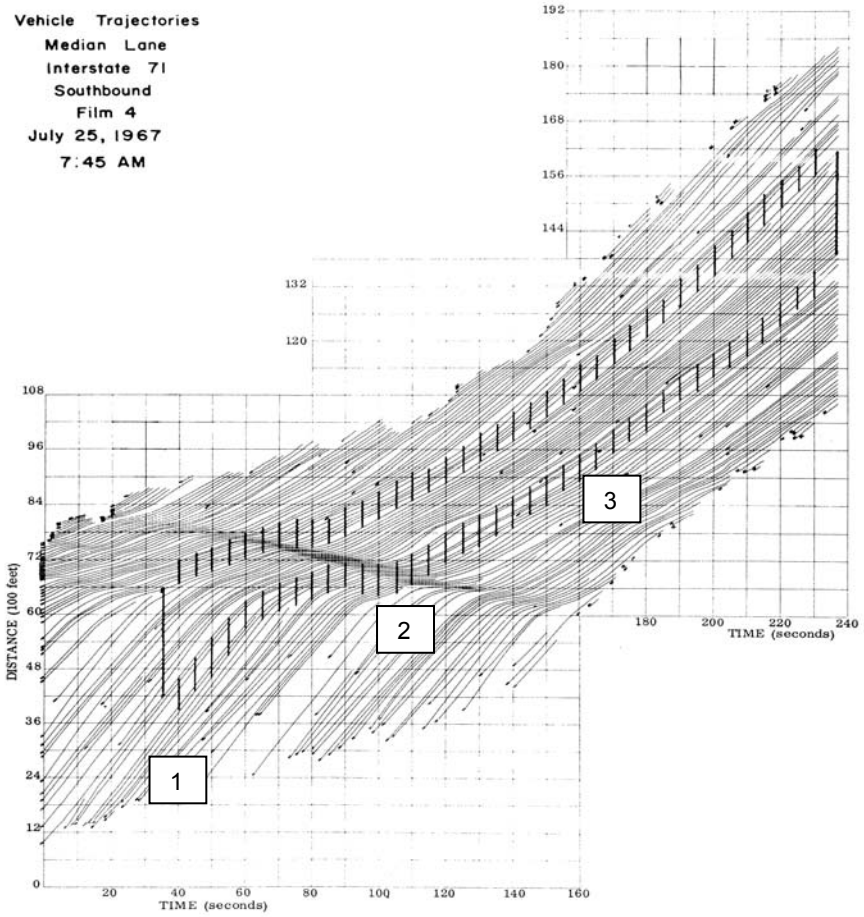

Figure 5-1 Traffic hysteresis phenomenon (Treiterer and Myers, 1974)

Based on the observation of Treiterer and Myers (1974), Zhang (1999) formulated the traffic hysteresis phenomenon to regenerate the double loop structure assuming three different phases of traffic: (1) anticipation dominant, (2) relaxation dominant, and (3)

anticipation–relaxation balanced phase as in Figure 5-2 (b). Zhang's model allowed a crossing between different phases in speed–density plane. Even more, according to his formulation, multiple crossing points can be made by allowing multiple loop structure.

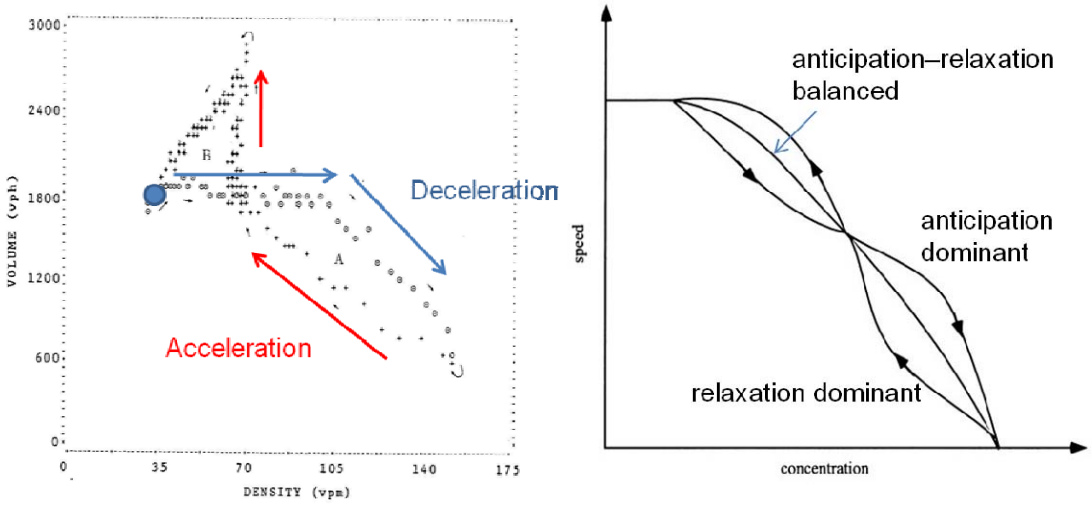

(a) Traffic hysteresis in Treiterer and Myers (b) Zhang's traffic hysteresis modeling

Figure 5-2 Traffic hysteresis modeling

Note that cycle 'A' is not a new finding, and is consistent with Edie's observations (1965), and Newell's theory (1965). But, cycle 'B', which has opposite direction and includes free flow traffic, has made some researchers to believe that the hysteresis phenomenon occurs between free-flow and congestion.

However, unfortunately, the observation on cycle 'B' was a suspicious one. First, the cycle 'B' had counter-clockwise loops, and the flow in speed recovery in cycle 'B' is higher than the flow when the traffic moves to congestion in cycle 'A'. Daganzo (1999) pointed out serious problems in data processing. Treiterer and Myers included lane changing vehicles, which affect the cycle 'B'.

Adding to Daganzo's criticism, we can also point out some problems. First, from free-flow conditions (100 kph, '1' in Figure 5-1) to congestion, transition ('2' in Figure 5-1) formed lower part of cycle 'B'. In other words, the traffic did not experience breakdown from the maximum flow but wave propagation from downstream. They are not part of hysteresis phenomenon and can be easily explained by the LWR theory. Secondly, as Daganzo pointed out, incoming lane changes ('3' in Figure 5-1) contributed forming of the upper right part of the cycle 'B', resulting in very high flow which is unusual. Finally, the platoon data, which are spatially averaged, include mixed traffic states of congestion and free flow making the data unreliable.

Even though, Treiterer and Myers (1974) attributed the cause of hysteresis to the asymmetry in acceleration and deceleration. Double loops with different directions arise for other reasons and need not to be explained in asymmetric theory. Therefore only cycle 'A' is of interest.

Figure 5-3 shows a speed-spacing relation for a vehicle from the NGSIM data. It shows the hysteresis phenomenon forming two cycles. Both cycles are counter-clockwise and won't appear as clockwise on the flow-density plane. As we can see, the cause of these cycles is the separation between acceleration and deceleration. In Figure 3-4, Figure 3-5, Figure 3-11, and Figure 3-6, we can see that **all** loops are counter-clockwise in the speed-spacing plane. Also, Figure 4-4 shows another example in platoon showing hysteresis phenomenon for the successive vehicles.

Recently, Laval (2008) also showed same perspectives on the traffic hysteresis phenomenon. He used six different sets of vehicle trajectory data including NGSIM data and the original data of Treiterer and Myers (1974). He traced the flow-density relationship

for platoons entering and exiting stop-and-go traffic, and found that there is no evidence of existence of cycle 'B'. Also, he showed that 66% of platoons (43% strong-level, 23% weak-level) have positive direction (clockwise in flow-density plane and counter-clockwise in speed spacing plane) hysteresis phenomenon, 20% negligible and 14% negative hysteresis. Comparing the negative hysteresis with the positive strong-level one, it seems that the negative hysteresis is not significant and can be classified to weak level which can be explained by stochastic behavior and vehicle mix. Thus, his result shows that hysteresis is mainly clockwise direction in flow-density plane, which supports asymmetric theory in platoon vehicles.

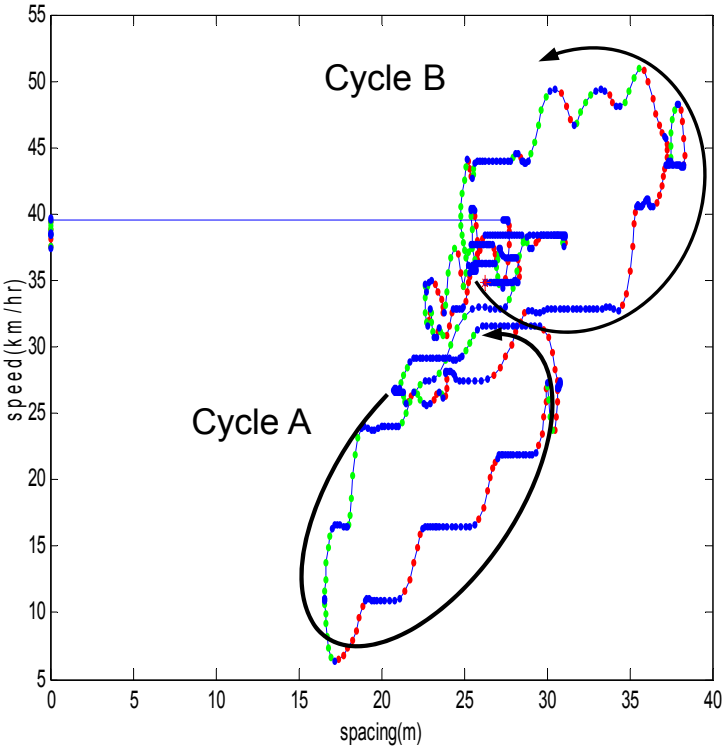

Figure 5-3 Traffic hysteresis phenomenon in NGSIM site

5.2 Traffic Stability

5.2.1 Stability in asymmetric theory

A traffic phase can be said to be stable if it persists for long time when there are no external causes, e.g., lane changes or changes in highway geometry which force change in traffic state. In other words, a vehicle's traffic state can be said "stable" if a small front gap reduction does not cause deceleration when the vehicle keeps constant speed. Figure 5-4 shows examples of stable and unstable traffic. We can see that in stable traffic, a small disturbance does not persist, but in unstable traffic, it causes wave propagation.

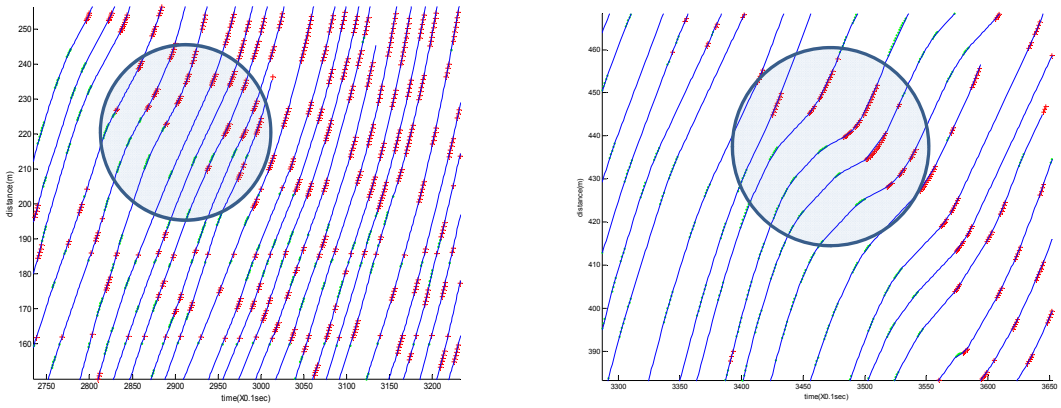

(a) Stable traffic (b) Unstable traffic

Figure 5-4 Traffic stability in NGSIM data

Traffic instability cannot be addressed in the macroscopic LWR model. Any disturbances, regardless of the size of impact, are propagated without being amplified in LWR model with parallel waves of deceleration and acceleration. Newell (1965) and Daganzo et al. (1999) used asymmetry to explain unstable traffic. They focused on the wave speed difference causing the disturbance wave to enlarge in time-space. With a small

disturbance of deceleration-acceleration pair with faster deceleration wave and slow acceleration wave, the influenced time periods of the disturbance wave are enlarged as the waves propagates upstream. The slow acceleration wave is due to coasting period between deceleration and acceleration.

In addition to the Newell and Daganzo's approach, we can focus on the impact of a spacing disturbance and the traffic phases. The impact can be defined as (resulting spacing –D-curve spacing), i.e., the remaining spacing to D-curve (Figure 5-5 (a)). When a small perturbation occurs, the driver in the following vehicle determines an appropriate action depending on the impact of the perturbation. If the impact is negative, the driver will start braking to move to the lower speed equilibrium region. If it is positive, he/she will keep his/her current speed. Therefore, the distance to the D-curve will determine the stability of the current traffic state of a vehicle.

In general, traffic near the D-curve (D-state) is relatively unstable because it is vulnerable to small perturbations, and easily moves to jam state. Traffic near the A-curve (A-state) is more stable, and a small disturbance can be absorbed when it meets near A-curve traffic. This argument also can help to understand stop-and-go traffic.

Kerner (1996b) claimed that the major reason for phase transitions, from free flow to congested "synchronized" states, is "spontaneous breakdown" which is caused by small disturbances. However, free flow is relatively stable, and it is very rare to have breakdown (i.e., substantial reduction in speed) in free-flow conditions without external causes. Ahn (2005) showed that most traffic breakdowns are caused by lane changing events in already congested traffic. In Figure 5-5 (b), "spontaneous breakdown" with small disturbance may only occur when the traffic state is region 'A' near D-curve.

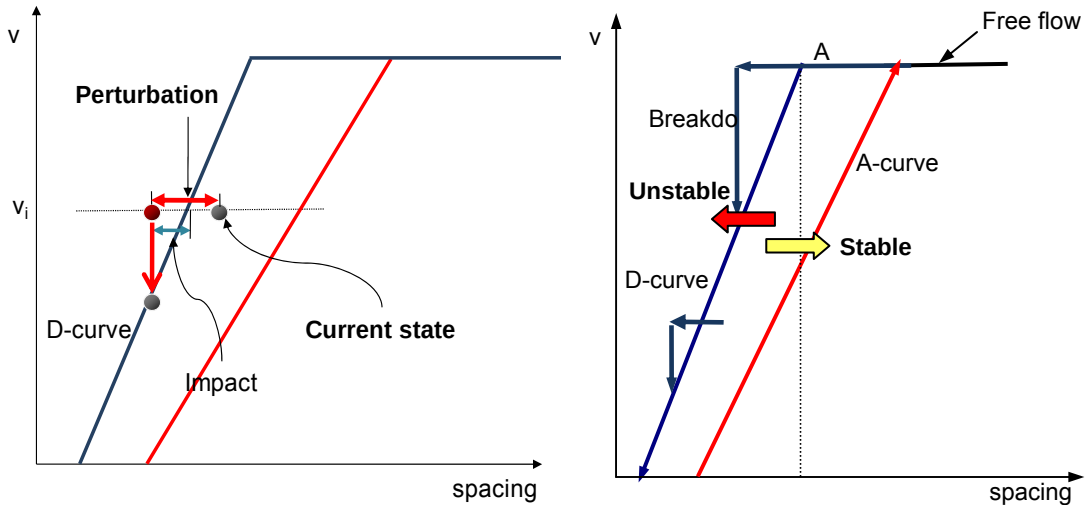

(a) Impact of a perturbation

(b) stability of traffic phases

Figure 5-5 Asymmetry and stability

5.3 Capacity Drop

"Capacity drop" is a reduction in discharge flow after queue formation, observed at downstream of an active bottleneck (Hall and Ageyemang-Duah, 1991; Banks, 1991, Cassidy and Bertini, 1999). Active bottleneck is characterized by queued upstream and free flowing downstream (Daganzo, 1997). Basically, discharge flow from active bottleneck is recovery flow from low speed congestion to high speed free-flow conditions. The reported drop in discharge flow varies among different sites. Bertini (1999) reported 12% drop in long run average, and recently Chung and et al. (2007) 3% to 18% flow reduction from its peak flow rate.

There arise two research questions concerning capacity drop phenomenon: a) why and how the capacity drop occurs? and b) how to predict the time and the amount of capacity drop?

The capacity drop phenomenon can be addressed by the discontinuity between free-flow and congested regions and empirical "reverse-λ" shape flow density relationship proposed by Koshi (1983). However, the mechanism of discontinuity between free flow and congestion has not been properly understood. Treiber et al. (2006) explained the capacity drop with "reverse-λ" shape flow density relationship and time headway variations. In this approach, they regarded the hysteresis phenomenon as a cause of capacity drop. But, they understood the hysteresis loop exists between the congestion and free flow, not between acceleration and deceleration.

Daganzo (2002) related the capacity drop to lane changing events in merging area. He addressed the mechanism of capacity drop in multi-lane traffic flow using two different groups of vehicles ("rabbits and slugs") which have different free flow speed and flow-density relationship. The low-speed slugs' lane changing behavior can limit the rabbits' high-speed behavior resulting in drop in discharge flow. From a microscopic view, Laval and Daganzo (2003, 2006) introduced limits in acceleration and maximum speed to explain the reason of capacity drop in lane changing situations. When a slow vehicle changes lane to the faster one, depending on the speed difference between lanes and acceleration capability, in some cases, it cannot catch up with the lead vehicle in the new lane, because of the acceleration limit and maximum speed limit resulting in very large spacing as vehicle '2' in Figure 5-6 (a). This explanation is valid for active bottlenecks in merging areas, where lane changes occur with large speed difference between lanes.

Adding to Daganzo's explanation above, in asymmetric theory, capacity drop can be understood as the difference of maximum flows of the two curves as shown in Figure 5-6 (b). Before the occurrence of the traffic breakdown, the flow has maximum value Q_{max}

which is on the D-curve. Once the bottleneck is activated, the maximum discharge flow, which is the recovery flow from upstream queue with lower speed, is Q_d lying on the A-curve as explained in Daganzo et al. (1999)

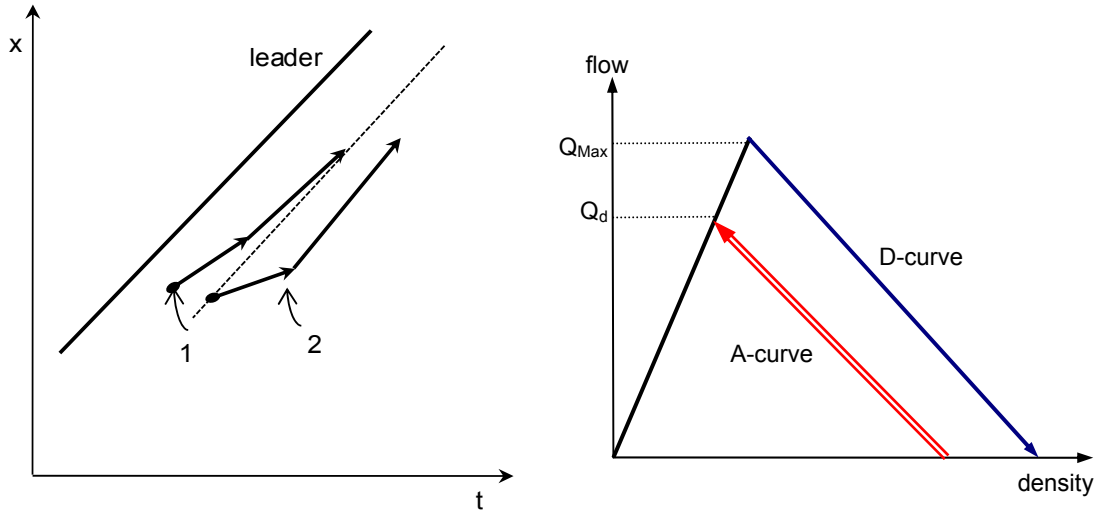

(a) Lane changing case (b) Asymmetry case

Figure 5-6 Capacity drop by lane changing and asymmetry

In freeway merging areas, stop-and-go waves are generated consecutively by incoming lane changes, and the vehicles experience slow-down as illustrated in Figure 5-7. After a vehicle passes the deceleration wave, traffic moves from the D-state (TD: trajectories following D-curve) with short gap to the A-state (TA: trajectories following A-curve) with larger gap. So, the discharge flow stays near the A-curve. Figure 5-7 (b) shows expanding trajectories when vehicles are passing deceleration waves. The dotted line between TD and TA is a virtual trajectory following Newell's simplified car-following model.

The amount of capacity drop varies according to the number of deceleration waves initiated by incoming lane changes and the number of lanes in the active bottleneck section.

This explains the wide variation in the amount of capacity drop reported from different sites in the literature. The relation of the capacity drop to the number of lanes and number of lane changes permits reliable estimates of capacity drop for active bottlenecks.

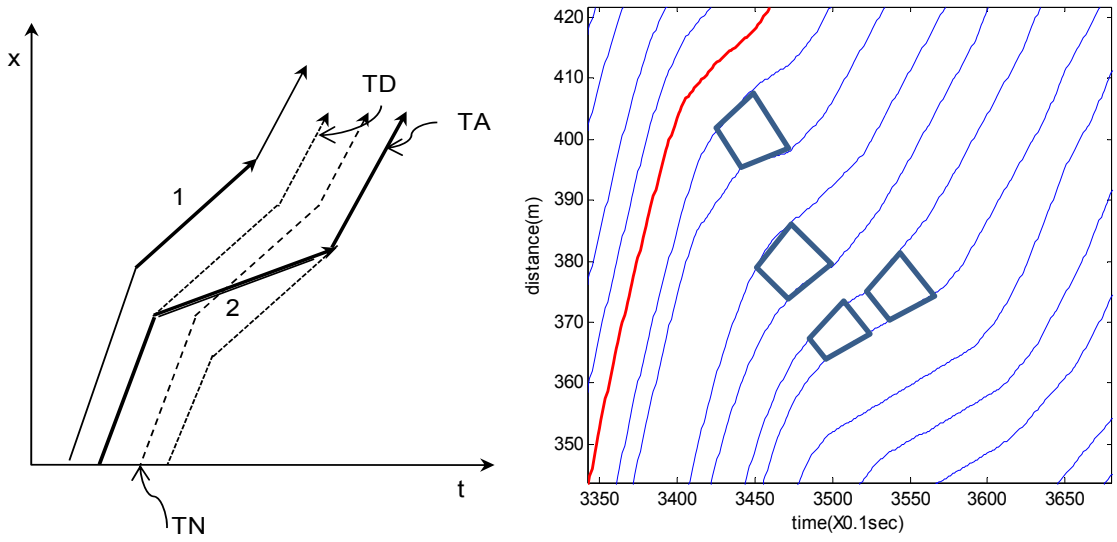

(a) Asymmetry case (b) Asymmetry case

Figure 5-7 Trajectories showing capacity drop

Drivers often try to adapt to the speed in the target lane during lane changing. This speed adaptation starts as soon as the driver decides to change lanes. When the original lane is slower than the target lane, the drivers usually keep short spacing, which is less than D-curve spacing, to catch up the target speed in the original lane. When they move to the new faster lane, they can change lane with very short spacing because when the leader is faster, they only needs the minimum jam spacing to secure safety as vehicle '1' shown in Figure 5-6 (a). This short spacing is relaxed later, a phenomenon known as relaxation after lane change (Cohen, 2004; Laval and Leclercq, 2008), which is discussed in the following section.

5.4 Relaxation Phenomenon after Lane Change

Cohen (2004) observed field data showing that both a lane changing vehicle and its follower in the new lane maintain very short gaps persistently for significant time period, which is called relaxation time, and then gradually increase the gap to a desired value. Because of the limitations of the field data, he couldn't determine the relaxation time period. His observations suggested that the relaxation time period is at least 15 to 20 sec or even longer. Hidas (2005) observed significantly short gaps after lane changing maneuver, for a period of about 6-10 sec. He proposed a model that allows gradual gap recovery process, by applying moderate/minimum deceleration instead of emergency braking to let the short gap increase gradually to the desired one. Laval and Leclercq (2008), using the NGSIM data, showed that the merging area has high density and the traffic returns back to normal density region after passing the merging areas.

Plots of vehicle trajectories from the NGSIM sites show that drivers keep very short spacing when they change lanes, and relax later depending on the traffic conditions resulting in larger spacing. Figure 5-8 shows the trajectories in lane changing in US101 site of NGSIM data which is a merging site located downstream of an on-ramp. Incoming lane changing vehicles are shown in thick line. Figure 5-9 shows trajectories of lane changing vehicles, and Figure 5-10 (a) and (b) each shows speed-spacing relation for the vehicle *n-1*, which changed lane at point '1', and vehicle *n*. With the lane changing action indicated as '1'' point, vehicle *n* starts deceleration. At point '2', vehicle *n-1* starts acceleration making the following vehicles to speed up. For vehicle *n*, the short spacing time period is about 15 sec, and for vehicle *n+1*, it takes less than 5 sec, and vehicle *n+2*, about 6 sec.

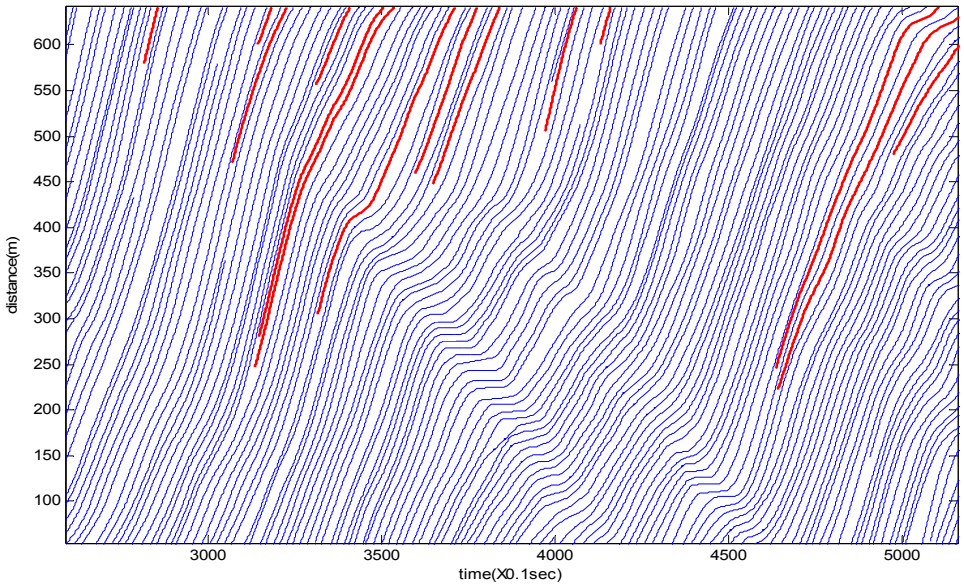

Figure 5-8 Lane changing in merging section, US-101, NGSIM

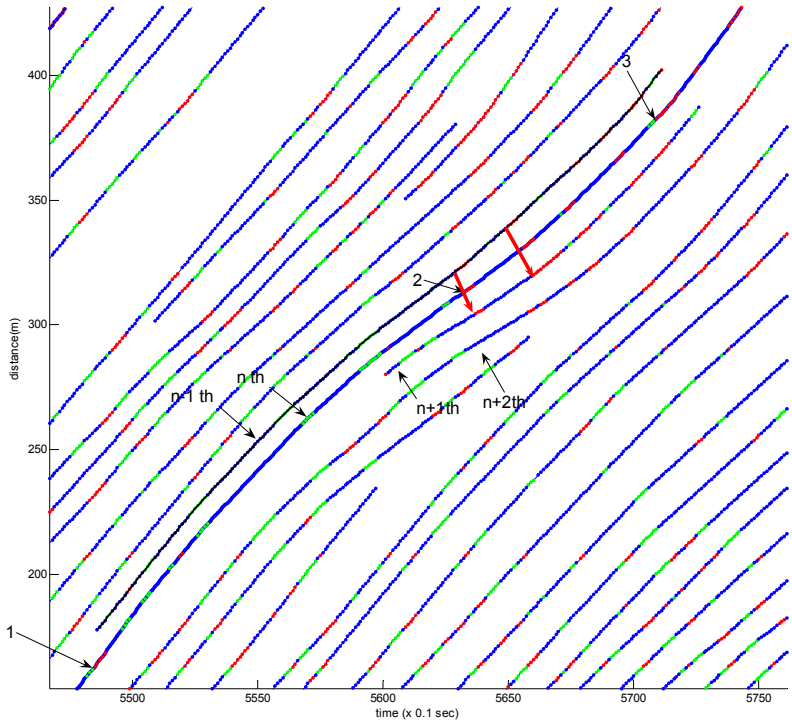

Figure 5-9 Vehicle trajectories in lane changing situation

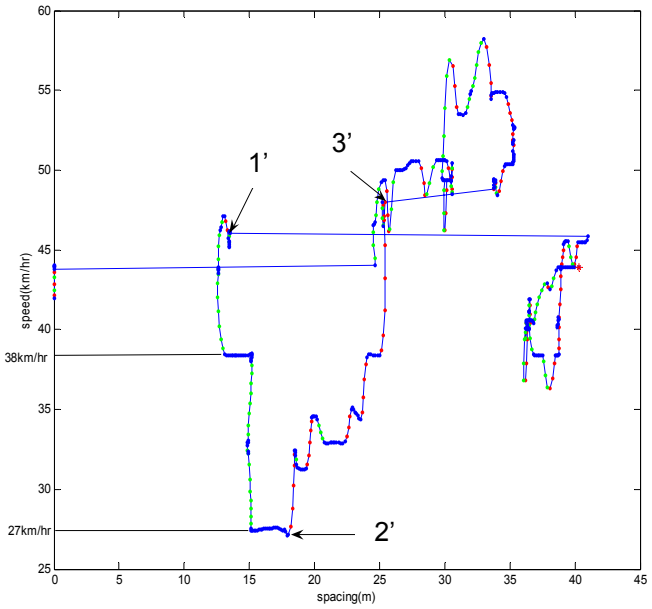

(a) Speed-spacing diagram of (n-1)th vehicle

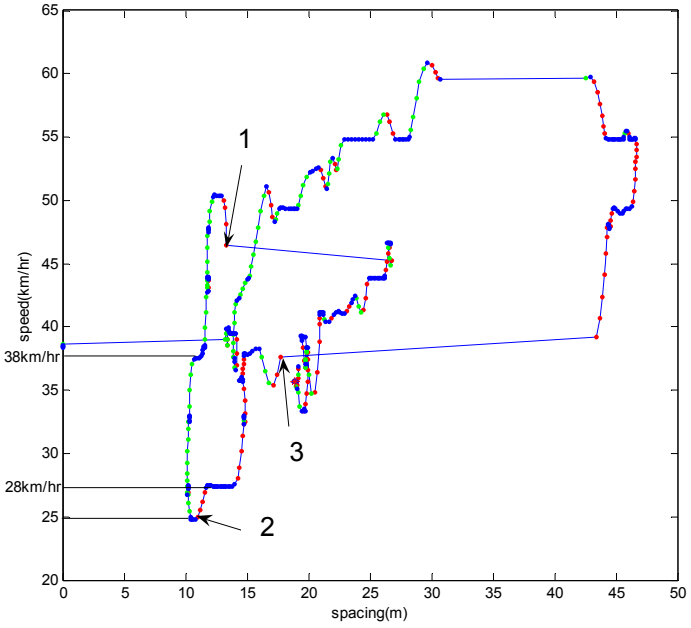

(b) Speed-spacing diagram of nth vehicle

Figure 5-10 Speed spacing relation in lane changing case.

In the proposed asymmetric theory the lane changing process has three stages as shown in Figure 5-12: (1) lane changing preparation (denoted as 'A'), (2) actual lane changing maneuver, and (3) returning to D-curve (denoted as 'B'). 'A' shows spacing adjusting for preparing imminent lane changes, in which drivers kept very short spacing less than D-curve spacing. When lane changes occurred, the vehicle already started deceleration. Following the lane change, path 'B' shows that the traffic phase is returning to D-curve. So the process 'B' is the relaxation process.[3]

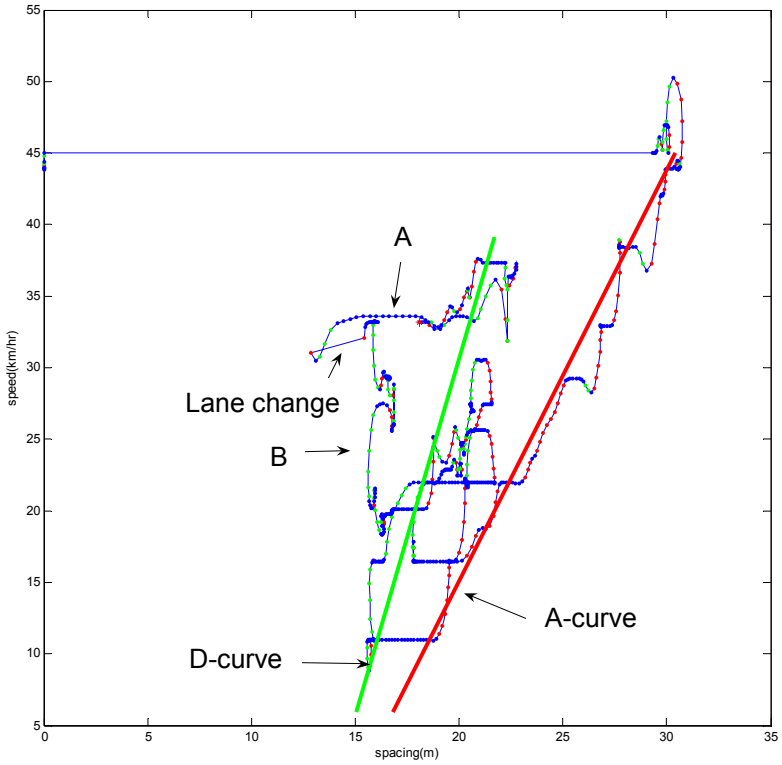

Figure 5-11 Lane changing in speed-spacing plane.

[3] Note that spacings are kept almost constant during the relaxation time period. In deceleration or acceleration, the driver tries to find a location on A or D-curve matching current spacing. Also, after the relaxation, the vehicle starts acceleration again to catch up with the leader's speed.

Therefore, the relaxation time period is dependent on the vertical time distance to the D-curve which can be calculated from the speed difference and spacing. If the incoming spacing of lane changing vehicle is large enough, greater than D-curve spacing, relaxation period is not needed.

Chapter 6 Application II: Understanding Stop-and-Go Traffic Phenomenon

In this chapter, we apply the proposed asymmetric traffic theory to explain the stop-and-go traffic phenomenon commonly observed in congested freeway traffic. The explanation is verified using examples from NGSIM vehicle trajectory data.

6.1 Introduction

Understanding the causes of stop-and-go traffic is important for modeling the formation and propagation of traffic jams and estimating the impacts of congestion. However, the mechanisms of the generation and evolution of the stop-and-go traffic in time and space have not been well understood yet, because of data limitations and theory deficiency. In order to reveal the detail mechanism of stop-and-go traffic, large quantities of microscopic data on individual vehicle trajectories on congested freeways are required. However, the acquisition and analyses of sufficient amount of trajectory data is very expensive and time consuming. The availability of the NGSIM database provides a unique opportunity to study in detail the stop and go phenomenon.

The stop-and-go traffic is closely related to the unexplained limitations of LWR theory mentioned in Chapter 2. In particular, the generation of stop-and-go traffic and how it is amplified in time and space can explain the unstable traffic flow and spontaneous breakdown. Also, the recovery flow from the stop-and-go traffic is directly related to the two-capacity problem. "Spontaneous breakdown" was suggested by Kerner (1996a, 1996b, 2002) as a main cause of the traffic breakdown from his observations. But, Daganzo et al. (1999) and Ahn and Cassidy (2007) have shown that the generation of stop-and-go waves can be traced back to lane changing events. This means that most of the stop-and-go traffic is related to lane changes, and the impact of the spontaneous breakdown on the generation of stop-and-go traffic is limited. Kerner (2004) proposed a qualitative three-phase traffic theory, in which the stop-and-go traffic is classified as the "wide moving jam". But, his proposed three-phase theory did not provide an explanation on the mechanism of the stop-and-go traffic, and it is not clear what causes the difference in driving behavior between the phases of "synchronized flow" and the "wide moving jam".

Schőnhof and Helbing (2007) classified congested traffic into 5 distinct states: moving localized cluster (MLC), pinned localized cluster (PLC), stop-and-go waves (SGW), oscillating congested traffic (OCT), and homogeneous congested traffic (HCT). The OCT and SGW states are related to the stop-and-go traffic. Similar to Kerner's approach, their classification is a phenomenological classification, and their microscopic mechanisms still remain unknown.

There also have been some efforts to model the stop-and-go traffic phenomenon. Applying Newell's (2002) simplified car-following theory, the trajectory of the following vehicle is always parallel to the lead vehicle, and the wave speeds of stop-and-go traffic are

same for both deceleration and acceleration for the same vehicle. In reality, it can be easily found that the trajectories in the stop-and-go traffic are not parallel, and the wave speeds for acceleration and deceleration are not same. In Del Castillo's model (2001), vehicle trajectories do not need to be parallel, but wave speeds are same (Figure 6-1). However, waves grow in dense traffic flow and decay in low density flow. Kim and Zhang (2004, 2008) used a stochastic gap time which change over time for each driver and causes different wave speeds for acceleration and deceleration, but still their vehicle trajectories are parallel (Figure 6-2). Both Del Castillo and Kim and Zhang noticed that the time headway distribution affects the future state of stop-and-go traffic, i.e. with larger headways, stop-and-go wave's decay, and short headway makes the waves grow. But, their approach is limited because they simply regarded time headway as random variable changing over time.

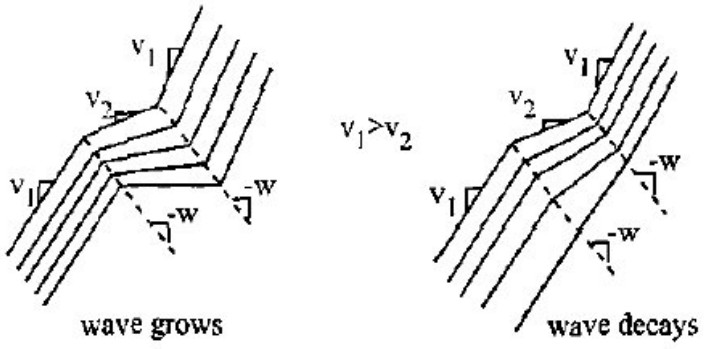

Figure 6-1 Dell Castillo's model

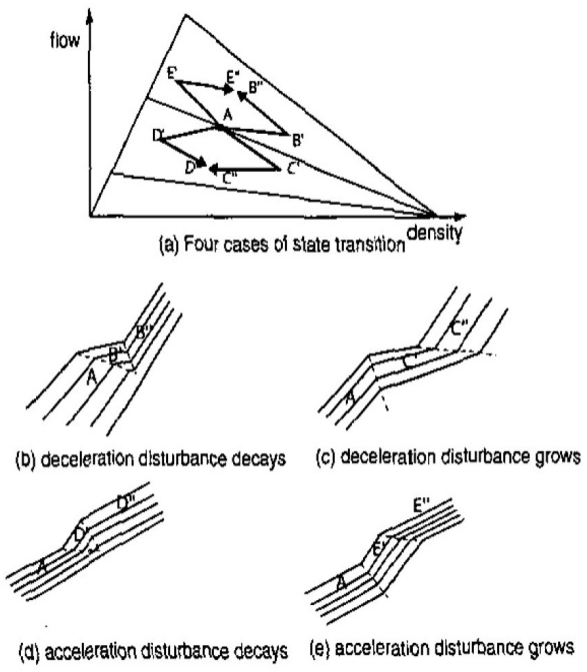

Figure 6-2 Modeling stop-and-go traffic (Kim and Zhang, 2004)

Returning to the Newell's initial asymmetric theory (Newell, 1965), he already provided a perspective on forming and dissipation of the instability (stop-and-go traffic inside congestion) using two-curves. Hereinafter, we will try to provide more detailed explanation and evidences based on the proposed theory from the previous chapters. The major improvements of the theory will be as follows:

1) Combining human behaviors of maneuvering errors and anticipation waves to improve the explanation of amplifying stop-and-go waves and diverse waves observed near stop-and-go traffic.
2) Detailed stop-and-go traffic mechanism with the proposed theory.

6.2 Life Cycle of Stop-and-go Traffic

In this section, we apply the proposed asymmetric traffic flow theory to explain the

stop-and-go traffic phenomenon. The key research questions relate to the life-cycle of stop-and go traffic, i.e., the understanding and explanation of the generation, growth and dissipation of traffic waves. Figure 6-3 shows vehicle trajectories illustrating these stages, and Figure 6-4 shows the life cycle based on the proposed theory.

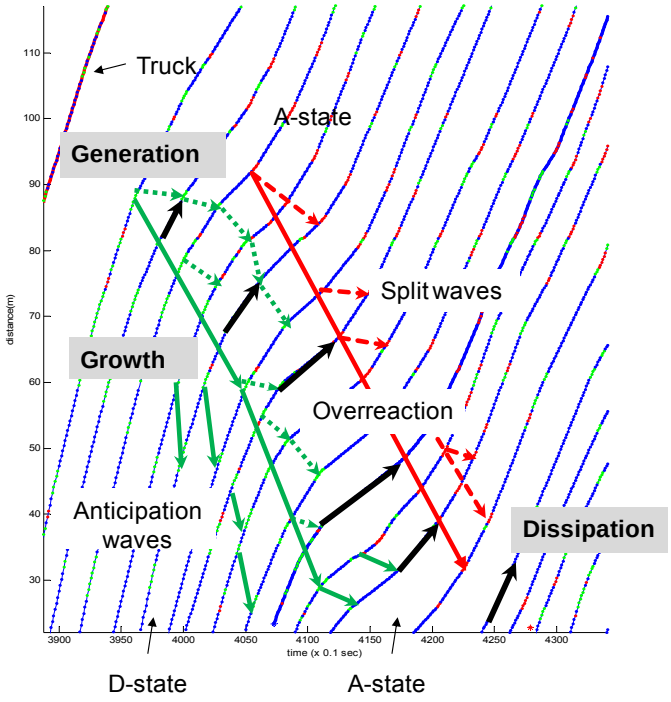

Figure 6-3 Life cycle of stop-and-go traffic, NGSIM example

Stop-and-go is generated near D-state (D-state is a state in which a vehicle is near D-curve or is decelerating, so it includes stationary and coasting phase near D-curve, and deceleration phase) in which traffic is decelerating or ready to decelerate because of the lower vehicle speeds downstream. In D-state, where vehicles drive in short spacing, a small disturbance can cause subsequent speed drops which may propagate upstream. As long as the upstream traffic is near D-state, the stopping wave of stop-and-go traffic grows and propagates upstream. This continues until the wave meets free flow traffic or vehicles

near A-state (A-state includes near A-curve stationary, coasting and acceleration phase), where vehicles have larger spacing which can absorb the stopping wave. When a vehicle in A-state meets a stopping wave, it will coast towards D-curve without braking, and then start deceleration according to speed difference. By delaying the braking event, the wave propagation is delayed and its speed decreases. Eventually, in A-state traffic, the stop-and-go waves dissipate, and the traffic will recover to higher speed state.

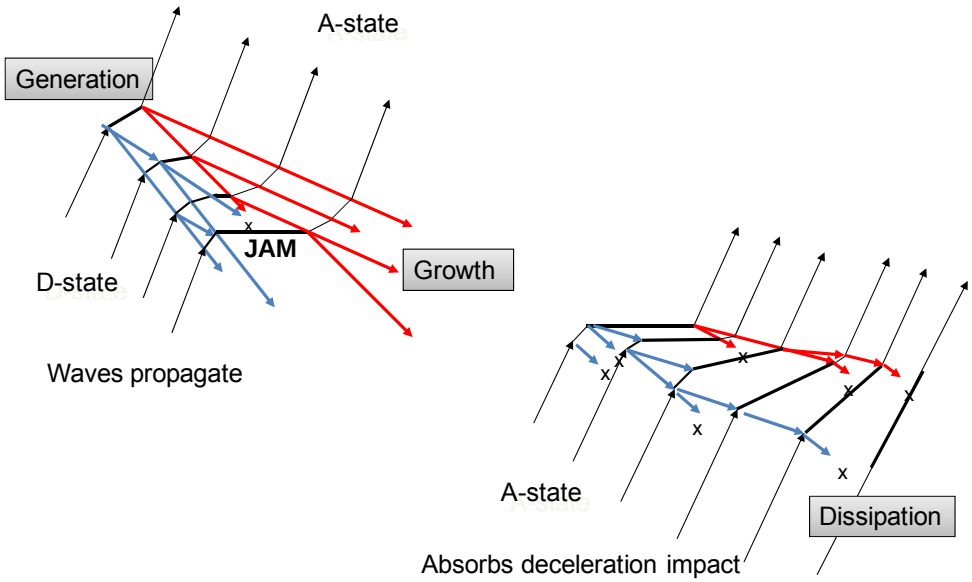

Figure 6-4 Life cycle of stop-and-go traffic

The mechanisms of stop-and-go traffic according to the stages of life cycle are described in detail in the following sections based on the proposed asymmetric traffic theory and driver behavior characteristics, notably over-reaction and anticipation.

6.2.1 Generation

Stop-and-go waves can be generated in unstable traffic which is near D-curve in congested traffic; also lane changing may cause stop-and-go waves as illustrated in Figure

6-5. But, the instability invoked in stop-and-go traffic is relatively small and cannot be propagated upstream unless the following traffic is also near D-curve; while the effect by lane changes are greater, and can propagate even the following traffic is not near the D-curve. This is the reason why stop-and-go waves are frequently observed to be formed near on-ramp merging areas. The location of stop-and-go traffic generation is expected to be close to lane changing locations. Also note that in Newell's theory, the deceleration path follows D-curve, while in the proposed one, it passes the D-curve first, and then moves down to the location on D-curve.

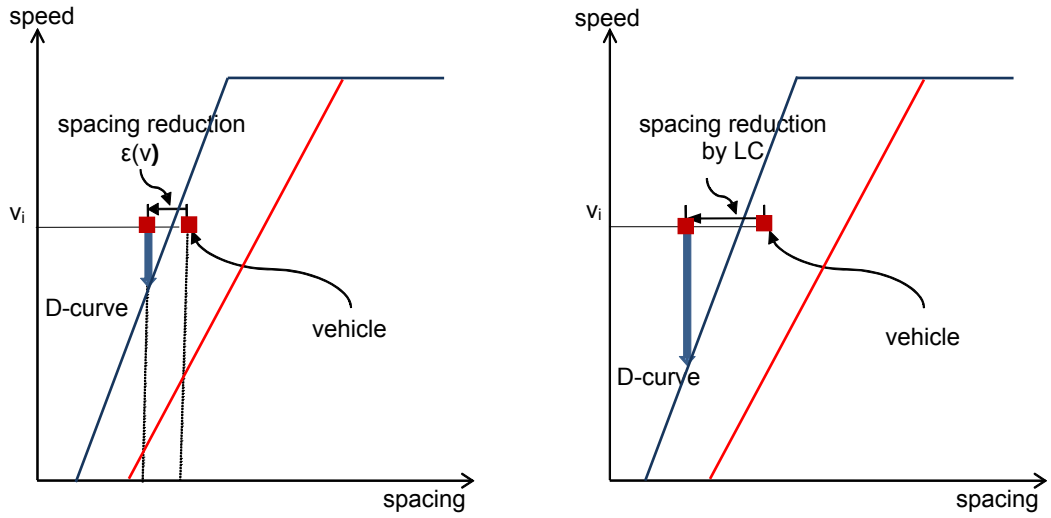

(a) Generation condition by instability (b) Generation case in lane change case

Figure 6-5 Generation condition of stop-and-go traffic

Figure 6-6 shows vehicle trajectories in congested traffic and illustrates the generation of stop-and go waves. Figure 6-6 (a) shows the example of stop-and-go generation by instability in congestion. In this case, the waves generated are short-lived with minimal impact. Figure 6-6 (b) shows the generation of waves due to lane changing. Before and immediately after the incoming lane changes, following drivers have to decelerate to yield

space to the lane changing vehicle generating stop-and-go waves. The recovery from the very short vehicle spacing following the lane change is known as the relaxation after lane changes (Laval and Leclercq, 2008), which also causes stop-and-go waves for about 5 to 20 seconds depending on the spacing after the lane change.

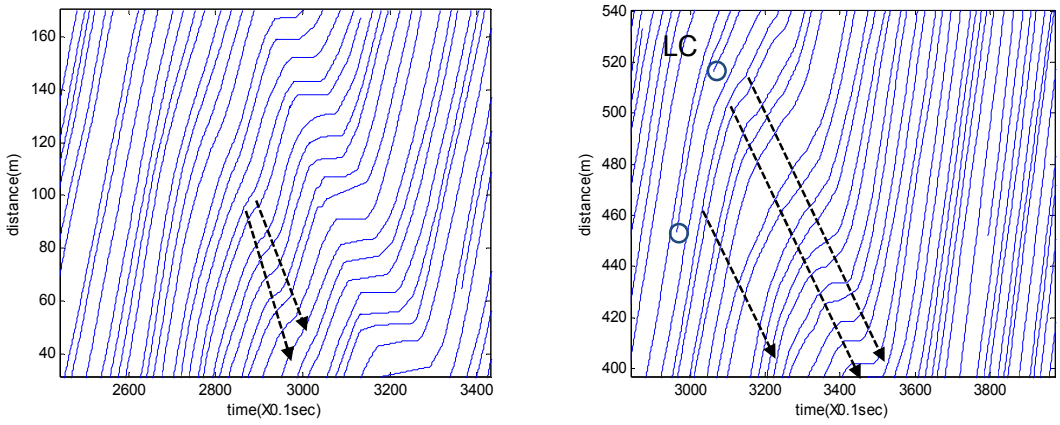

(a) stop-and-go generation by instability (b) the generation by lane changes.

Figure 6-6 Generation of stop-and-go traffic

6.2.2 Growth

The mechanism of the growth is basically same with the one of generation. Here, the focus is on the amplification of the waves. When the traffic state is near D-curve, a small disturbance can propagate and be amplified combined by over-reaction and anticipation effect as described in the previous section. There are some distinct phenomena in the growth phase, including a) drop of minimum speed (amplification), b) expansion of the affected time period, and c) fast running anticipation waves.

Figure 6-7 (a) illustrates the trajectories in growth state, and (b) shows an example of measured trajectories from the NGSIM dataset. In the Figure, 'TD' (D-curve Trajectory) represents the expected D-curve trajectories when the driver keeps D-state, and 'TA'

(A-curve trajectory) is the expected A-curve trajectories. Because a transition from D-curve to A-curve is required in growth stage before exiting stop-and-go waves, the minimum speed always drops compared to the minimum speed of the leader vehicle, and the acceleration wave is usually delayed ('C'→'B', in Figure 6-7 (a)). The transition period depends on the speed of the '2'- minimum speed. It is determined by the proximity to the D-curve, i.e., the closer to the D-curve, the more the driver has to decelerate to reach 'TA'.

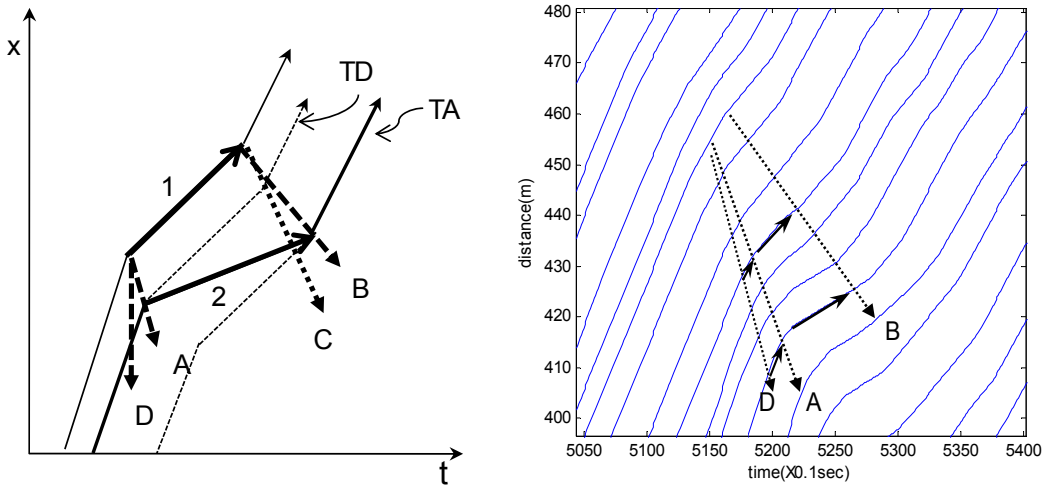

(a) Growth of stop-and-go traffic (b) NGSIM example of stop-and-go traffic growth

Figure 6-7 Growth of stop-and-go traffic

If the minimum speed is too low because of maneuvering errors, the wave 'B' can be faster than wave 'C'. It is also possible that drivers intentionally lower the minimum speed to make a faster transition from the state near D-curve to the state near A-curve. Because drivers want to exit stop-and- go waves as quickly as possible, this action is attractive to some drivers. This intention also can be fulfilled by anticipation. If the driver's view is not restrained, for example in the presence of tall vehicles, he/she may begin decelerating earlier before meeting wave 'A', and the traffic state can move to near A-state quickly, or he can maintain higher speed during the deceleration period. In Figure 6-7, 'D' represents

the anticipation wave which also enlarges the affected time period. So, the growth of the stop-and-go waves is a process determined by the anticipation, D-curve proximity, and car-following behavior. Figure 6-8 shows some sample trajectories in growth stage of stop-and-go traffic. Note that vehicle '7' was approaching a stop-and-go traffic with very short spacing represented as small triangle which represents reaction time and jam spacing. The vehicle '7' can be thought first to be in the D-state traffic following 'TD', which is shown as small triangles and then after passing the stop-and-go traffic, it follows 'TA'. The bigger triangles show that vehicle '7' moved to A-state traffic. The trajectories in the box show the transition from D- to A-state traffic. It shows the characteristics conforming to the theory developed here. Same phenomena also occurred in case of the vehicle '2', '3', '5', and '6'. Note that when vehicle '4' passed the stop-and-go wave, the minimum speed was recovered; the wave was in dissipation stage not in growth stage.

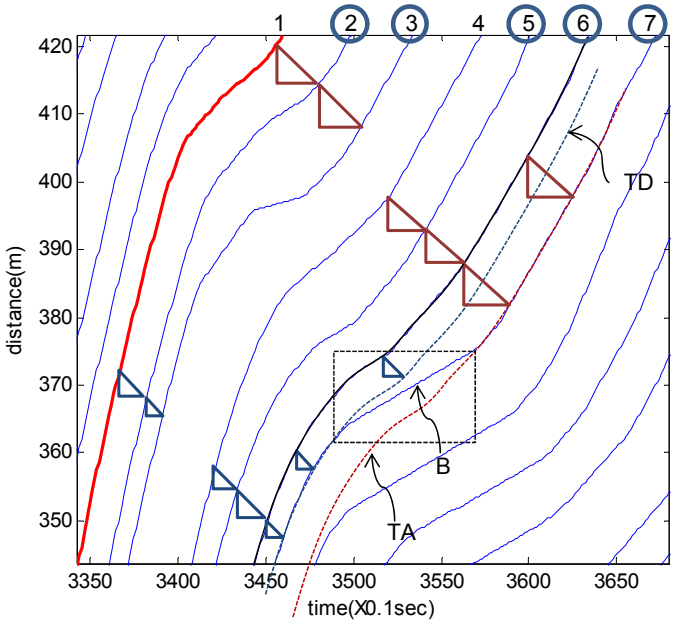

Figure 6-8 Growth of stop-and-go traffic

6.2.3 Dissipation

When a vehicle's traffic state is near the A-curve or in free flow, it can absorb the impact of stop-and-go traffic. If the front spacing reduction by stop-and-go traffic is less than the distance to the D-curve as shown in Figure 6-9 (a), the impact of spacing reduction will be reduced or entirely eliminated. So, if the following traffic is near the A-curve, the stop-and-go traffic waves will dissipate. In Figure 6-9 (b), keeping large spacing, vehicle '2' can absorb the spacing reduction impact, and all the waves stop to propagate. After absorbing the stop-and-go waves the vehicle will move closer to the D-curve state. Meeting another stop-and-go waves, it can easily breakdown. Inside congested traffic, A-curve traffic can be generated after passing a stop-and-go traffic. If a front vehicle exits or changes lane to other lane, the following vehicle can also be near in A-curve. There are distinct phenomena in dissipation including a) minimum speed recovery, b) reduction of the affected time period, and c) deterred wave or wave elimination.

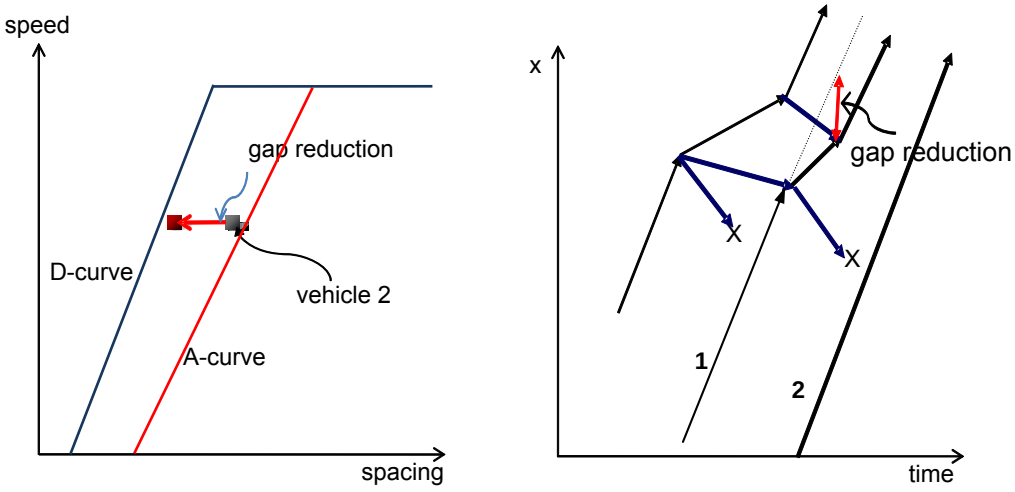

(a) Dissipation condition in speed-spacing relation. (b) Stop-and-go dissipation with discontinued deceleration waves in time-space.

Figure 6-9 Dissipation of stop-and-go traffic.

When the spacing reduction impact is reduced, minimum speed can be recovered (‘1’→ ‘2’ in Figure 6-10 (a)), and the deceleration wave can be delayed during the coasting phase from A-curve to D-curve (wave ‘C’→wave ‘A’). Figure 6-10 (b) shows an actual example of stop-and-go dissipation showing the above characteristics. Passing wave ‘A’ and ‘B’, drivers have wide range of choice. Passing wave ‘A’, the driver can choose the amount of deceleration. The shaded area in the Figure 6-10 (a) shows the possible range of trajectories. Passing wave ‘B’, combined with anticipation of the downstream traffic, the driver can choose the point and the amount of acceleration.

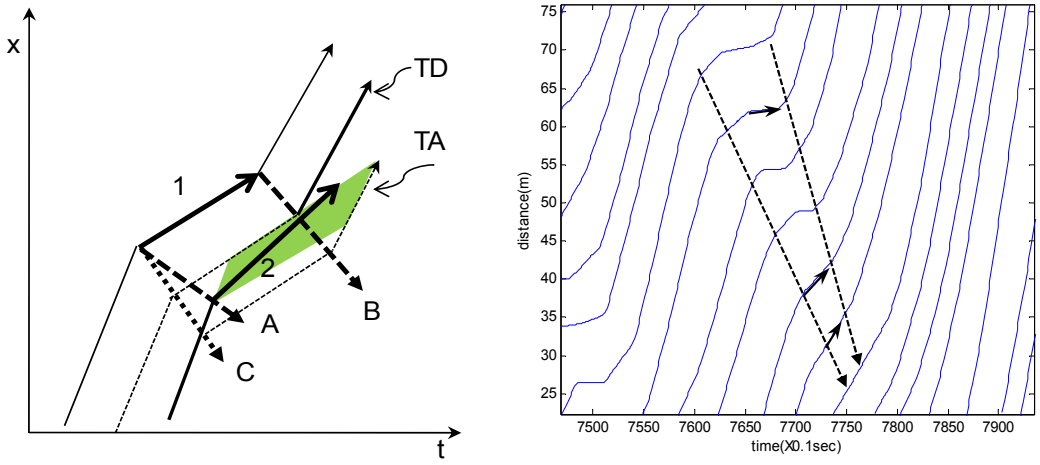

(a) Dissipation (b) NGSIM example

Figure 6-10 Dissipation of stop-and-go waves

Figure 6-11 (a) shows the phase changes during the dissipation stage. Passing the waves, traffic phases changes near A-state (big triangles) to near D-state (small triangles) which has short spacing and less wave travel time. It can be explained that anticipation of acceleration plays main role in the spacing changes in dissipation stage. After passing the waves, anticipating future speed recovery, drivers do not return to A-state and keep staying nearer to D-curve for faster travel.

As incoming lane changes make the stop-and-go waves grow, outgoing lane changes make the stop-and-go traffic decay by moving the traffic phase of the following vehicle to A-state that can absorb the impact of stop-and-go traffic. Figure 6-11 (b) shows an example of stop-and-go traffic dissipation by lane changes.

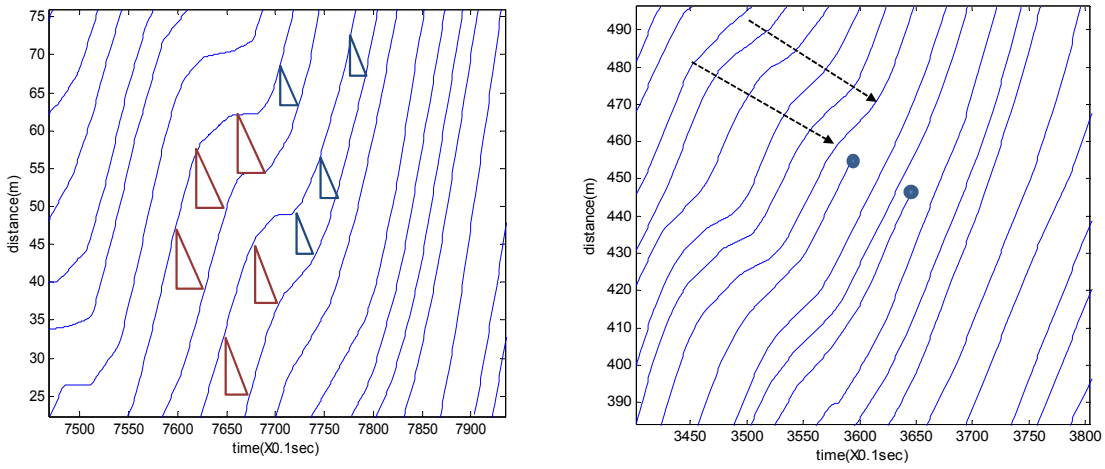

(a) Dissipation (b) Dissipation by lane change

Figure 6-11 Dissipation of stop-and-go waves

6.3 Interaction of Waves in Stop-and-go Traffic

Stop-and-go traffic involves several waves: anticipation wave, deceleration and acceleration waves, and secondary waves split from other waves (Figure 6-3 and Figure 6-12). Waves with different speeds may collide. In case of collision of acceleration and deceleration waves, the two waves can cancel out. If waves of the same kind meet, the impact can be amplified. In Figure 6-12 (b), cross (+) symbol represents acceleration point and circle (•) symbol is for deceleration point. The waves denoted as '1' are anticipation waves. Wave '5' shows split waves. The acceleration at point 'b' can be explained by the arrival of anticipation wave considering its fast propagation speed or by the effect of the

secondary wave split from the wave arriving at point ‘a’. In case that the wave ‘4’ is an anticipation wave, the wave ‘3’ and ‘4’ collide at point ‘b’, and the amount of acceleration is determined by the combined impact of waves ‘3’ and ‘4’. If anticipation is not involved at the point ‘b’, the wave ‘2’ actually works as an acceleration wave because of the over-reaction done at point ‘a’, and the wave ‘3’ cancels out by wave ‘2’.

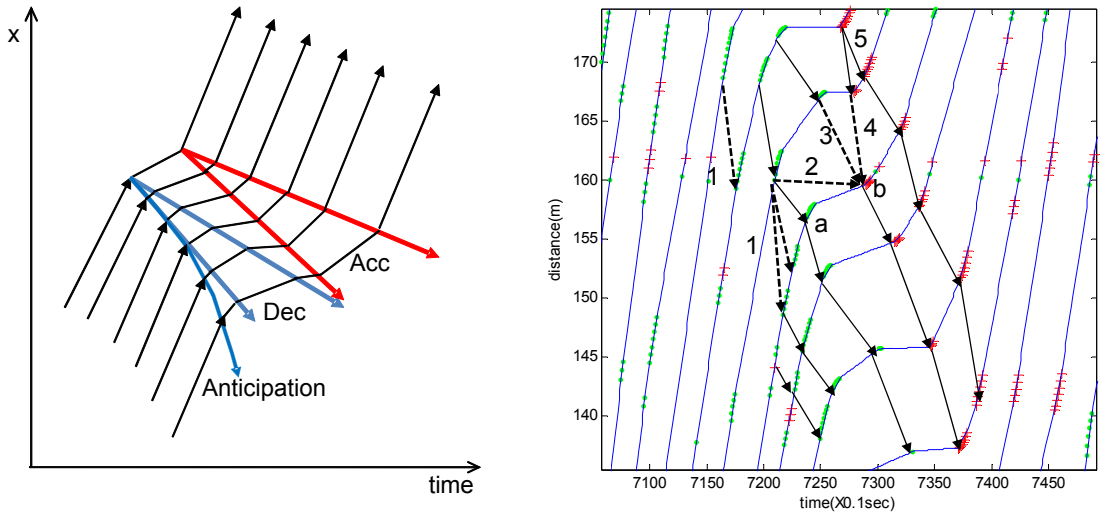

(a) Waves involved in the stop-and-go traffic (b) waves propagation in US-101 site.

Figure 6-12 Stop-and-go waves

When multiple stop-and-go waves occur in a nearby location, waves usually run parallel because of the similar speeds as shown in Figure 6-13. However, the stop-and-go traffic downstream (denoted as ‘C’, ‘D’ and ‘E’) can be influenced by the upstream conditions (‘A’, ‘B’). When vehicles pass stop-and-go waves, their traffic phase can change. In passing the growth stage stop-and-go traffic, the traffic phase usually changes from the D-state (near the D-curve state) to the A-state (near the A-curve state). In the dissipation stage, the traffic phases can change from the A-state to the D-state. Figure 6-13 shows how the change in traffic phase affects the stop-and-go traffic downstream. Wave

'A' is generated due to several lane changing events ('1', '2', '3', '6', '7', and '8'). Passing wave 'A', the traffic phase changes to A-state, which influences wave 'C' generated by two lane changing events, '4' and '5'. As the A-state traffic meets a second wave, it absorbs the stop-and-go impact of the second wave, and causes dissipation. 'D' shows the dissipating wave. After passing wave 'B', the traffic states changes from A-state to D-state causing the growth of wave 'E' from the weakened wave 'D'.

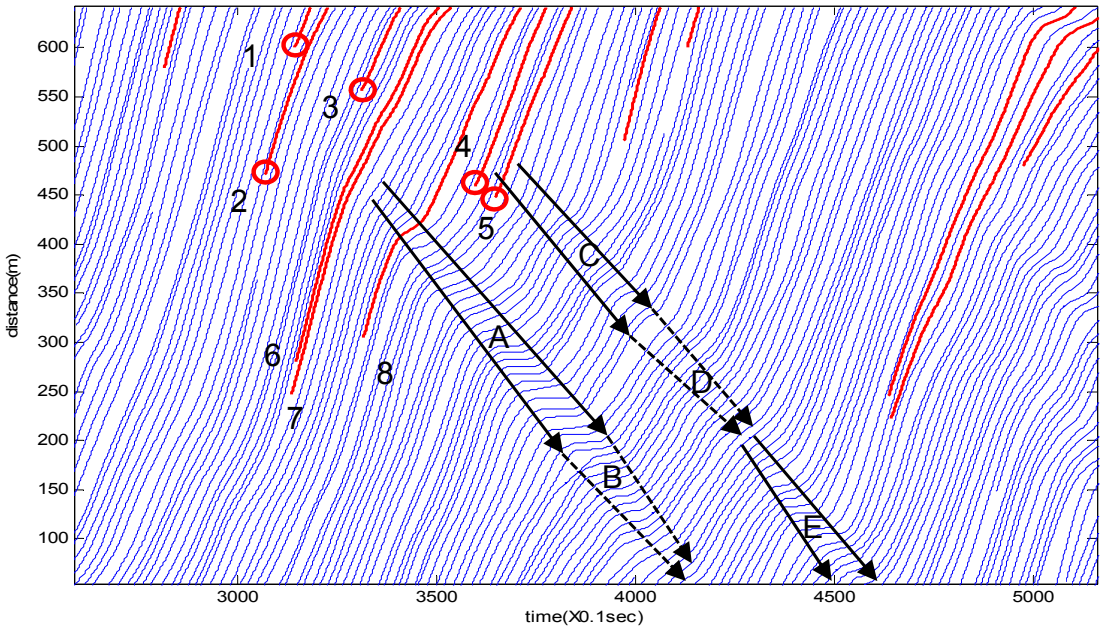

Figure 6-13 Stop-and-go waves' evolution in time space.

6.4 Smoothing Out of Stop-and-go Waves

Split waves and anticipation waves also enlarge the affected time period as the waves propagate upstream as shown in Figure 6-14. This enlargement "smoothes out" the original impact of speed change enabling following drivers' gradual speed adjustment. Thus, when a sharp impact is smoothed out, the upstream traffic experiences speed drop with

stop-and-go traffic's gradual dissipation. Although the smoothing out effect is mainly caused by the anticipation wave, not all drivers will have anticipation. In case that the sight of the drivers are limited or the stop-and-go traffic has short width in time so that the detection of front stop-and-go traffic is difficult, stop-and-go traffic will be amplified rather than smoothed out. In Figure 6-14, meeting several stop-and-go waves ('1', '2', '3', '4', '5'), vehicles' speed in region 'B' is much less than the original speed in region 'A'. Thick lines show lane changing vehicles. Dotted lines represent reference speed in region 'A', positive solid arrows represent speed of traffic and negative arrows are for the stop-and-go waves.

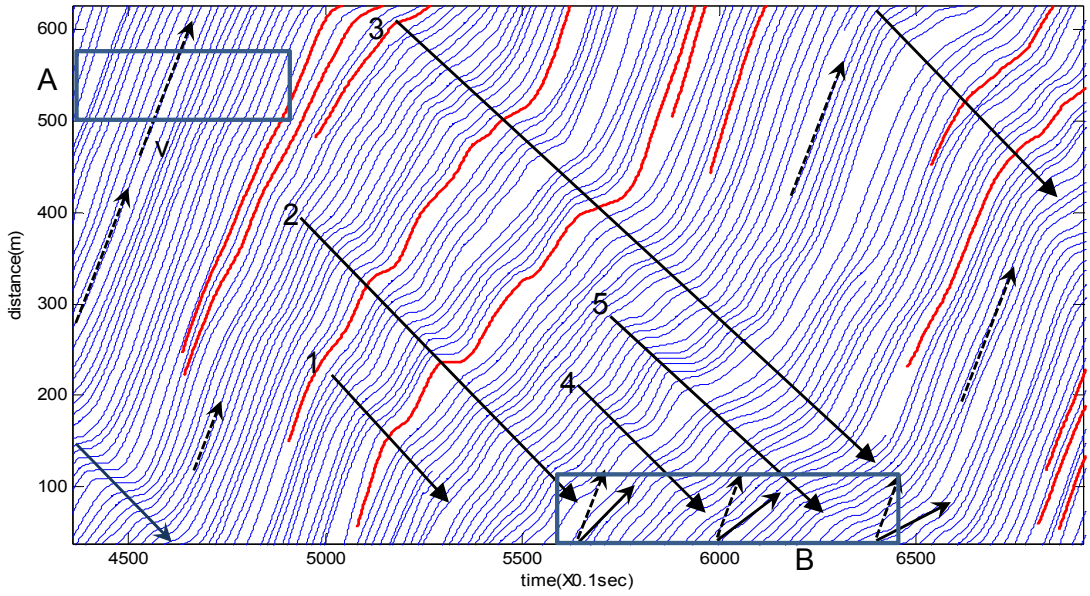

Figure 6-14 An example of smoothing out of stop-and-go waves in US-101 site.

Chapter 7 Microscopic Fundamental Diagram

This Chapter is a speculation on the shape of the A/D-curve using safety constraints. It describes a model incorporating the asymmetric microscopic driving behavior theory proposed in Chapter 3. As boundaries of stationary phase, A-curve and D-curve models describe the fundamental relationship in speed-spacing plane at the microscopic level. Here, we will derive a microscopic Fundamental Diagram (mFD) consisting of A-curve and D-curve using basic Newtonian equations.

Assume that two vehicles (leader and follower) are running at constant speed (v) and spacing (s), what we want to derive is the lower bound and upper bound of the spacing for speed v which does not need any action. At current time, the trajectories are parallel and the speeds of the two vehicles are same. Assuming the worst case scenario of leader vehicle's full stop from the current time, the following has to start a full stop after its reaction time.

During the reaction time period from current time to reaction time, we can assume that the follower can be decelerating (D), coasting with current speed (C) or accelerating (A). Let the safe spacing for each case S_D, S_C and S_A. Note that $S_D \leq S_C \leq S_A$. For safety's sake,

the current spacing $S \geq S_D$, S_C. Therefore, D-curve can be derived by calculating S_C which is the maximum spacing that allows current spacing to be safe without any action for the reaction time period even in this worst situation. If the current spacing $S \geq S_A$, the follower can accelerate without having sacrificing safety constraint. So, spacing $S \geq S_A$ is unnecessary. Therefore, A-curve can be derived by calculating S_A.

7.1 D-curve Formulation

7.1.1 D-curve model derivation

A deceleration model can be derived from the safety distance calculation in car-following based on the approach suggested by Gipps (1981). In stationary car-following state, a following vehicle has to keep minimum safe driving spacing for a given speed. Safe driving spacing for speed *v* is the minimum spacing, which guarantees that the following vehicle can avoid front-end collision even in the worst case of lead vehicle's emergency braking if both lead and following vehicle are in stationary state.

Assume that a lead vehicle *n-1* starts a full stop at time *t*. The following vehicle *n* will react τ seconds later, and start braking at the maximum rate. After a full stop with maximum deceleration, the spacing still must be greater than jam spacing value (Figure 7-1).

The stopping distance *d* for each vehicle can be written as equation (7-1), where, subscript *n* denotes the following vehicle, and *n-1* the lead vehicle.

$$d_n(t) = -\frac{\left(v_n(t+\Delta t)\right)^2}{2a_n^L}, d_{n-1}(t) = -\frac{\left(v_{n-1}(t)\right)^2}{2a_{n-1}^L} \quad (7\text{-}1)$$

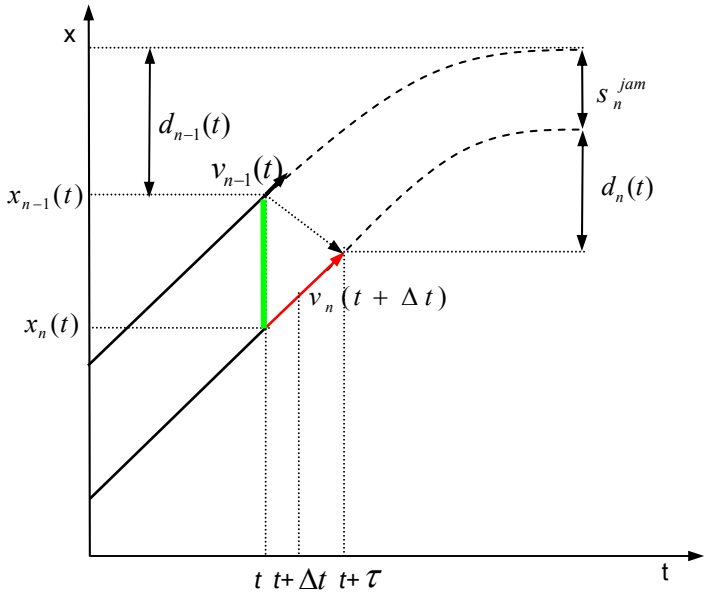

Figure 7-1 Safety driving spacing in deceleration

The safety constraint for the following vehicle can be written as follows:

$$x_{n-1}(t) + d_{n-1}(t) \geq x_n(t) + v_n(t+\Delta t)\tau_n + d_n(t) + s_n^{jam} \tag{7-2}$$

$$x_{n-1}(t) - x_n(t) \geq v_n(t+\Delta t)\tau_n + d_n(t) - d_{n-1}(t) + s_n^{jam} \tag{7-3}$$

Replacing the left hand side with safety spacing, we get:

$$s_n^D(v) = v_n(t+\Delta t)\tau_n - \frac{(v_n(t+\Delta t))^2}{2a_n^L} + \frac{(v_{n-1}(t))^2}{2a_{n-1}^L} + s_n^{jam} \tag{7-4}$$

Assuming stationary case, when the two vehicles' speeds are same at time *t*, and the following vehicle keeps its speed for τ , then we can obtain spacing function $s^D(v)$.

if $v = v_n(t+\Delta t) = v_{n-1}(t)$

$$s_n^D(v) = v\tau_n + (\frac{1}{2a_{n-1}^L} - \frac{1}{2a_n^L})v^2 + s_n^{jam} \tag{7-5}$$

Where,

s_n^{jam} : Jam spacing, a_{n-1}^L : Maximum deceleration of vehicle *n-1,*

a_n^L : Maximum deceleration of vehicle n

For Equation (7-5) shows the relation between the speed and minimum safety spacing for deceleration, s^D is the D-curve spacing for given speed.

7.1.2 D-curve for homogeneous and inhomogeneous traffic

In homogeneous flow case, i.e., both vehicles have same deceleration rates, the v^2 term equation (7-5) is cancelled out and the most familiar equation (7-6) is obtained, which is Newell's simplified car-following model:

$$s_n^D(v) = v\tau_n + s_n^{jam} \tag{7-6}$$

Curve (a) in Figure 7-2 shows a homogeneous case, and curve (b) shows an inhomogeneous case when the following vehicle has lower deceleration capability than the lead vehicle, e.g., truck following a passenger car case (auto-truck). As case (b) in Figure 7-2, it needs more spacing than auto-auto (passenger-passenger) case as the speed increases.

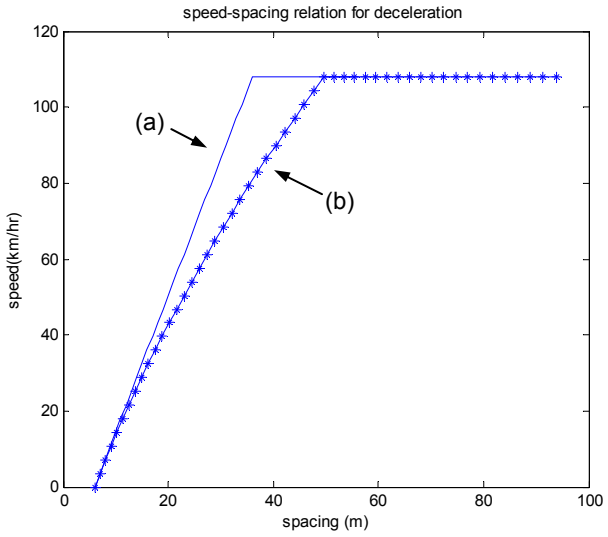

Figure 7-2 D-curve model for homogeneous (auto-auto) and auto-truck case

In deriving equation (7-5), we considered full stopping case, which is actually an extreme case. We can replace the maximum deceleration rate of the following vehicle with nominal deceleration which is a preferred deceleration rate in driving:

$$s_n^D(v) = v\tau_n + (\frac{1}{2a_{n-1}^L} - \frac{1}{2a_n^d})v^2 + s_n^{jam} \quad (7\text{-}7)$$

Where,

a_n^d : Nominal deceleration rate for nth vehicle.

Equation (7-7) is the preferred speed-spacing relation in deceleration process.

7.2 A-curve Formulation

7.2.1 A-curve model derivation

An acceleration model can be derived using a similar approach as in deceleration model. Drivers want to keep safe and comfortable spacing that allows acceleration without collision when the lead vehicle suddenly stops. Figure 7-3 shows this situation. If the following vehicle plans accelerating from time *t* with the lead vehicle's full stopping from time *t*, it will start decelerating to a full stop at time $t+\tau$ to prevent collision. And the spacing after stopping must be greater than jam spacing. So, the spacing *s* ensures safety even if a driver starts accelerating and the lead vehicle makes a sudden stop. If the spacing is greater than this value, it is unnecessary and the driver can speed up for faster travel.

Assuming the following vehicle's acceleration applied from time *t* for τ_n, the following vehicle maintains accelerating during this time period. Assume that the maximum acceleration, a_n^U, was applied for τ_n seconds.

$$x_{n-1}(t) - x_n(t) \geq v_n(t)\tau_n + \frac{a_n^U \tau_n^{\,2}}{2} + d_n(t) - d_{n-1}(t) + s_n^{jam} \tag{7-8}$$

Arranging for minimum safe spacing, Equation (7-8) gives:

$$s_n^A(v) = v_n(t)\tau_n + \frac{a_n^U \tau_n^{\,2}}{2} - \frac{\left(v_n(t+\Delta t)\right)^2}{2a_n^L} + \frac{\left(v_{n-1}(t)\right)^2}{2a_{n-1}^L} + s_n^{jam} \tag{7-9}$$

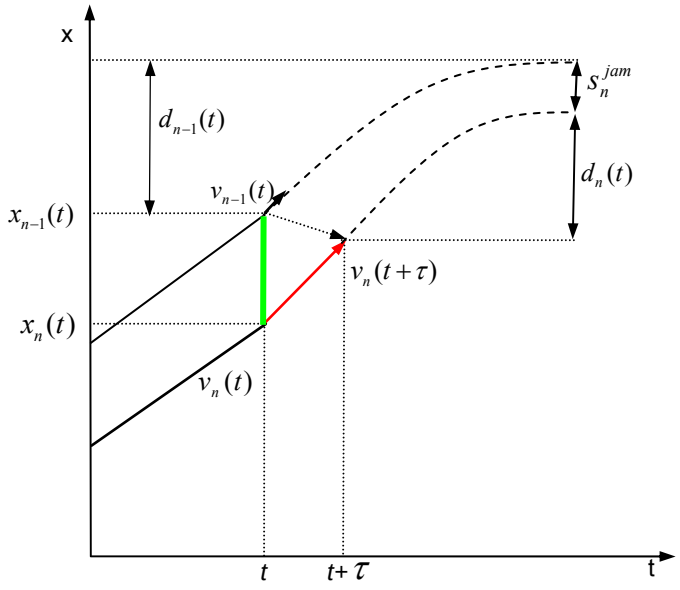

Figure 7-3 Safety driving spacing in acceleration

The spacing must satisfy the constraint in equation (7-8) which is identical with equation (7-3), except the speed in the next simulation time step.

Assume that the traffic is stationary, the equations (7-10) and (7-11) are obtained.

if $v_{n-1}(t) = v_n(t) = v$

$$s_n^A(v) = v\tau_n + \frac{a_n^U \tau_n^{\,2}}{2} - \frac{\left(v + a_n^U \tau_n\right)^2}{2a_n^L} + \frac{v^2}{2a_{n-1}^L} + s_n^{jam} \tag{7-10}$$

$$s_n^A(v) = v\tau_n + s_n^{jam} + \frac{a_n^U \tau_n^{\,2}}{2} + \frac{v^2}{2a_{n-1}^L} - \frac{\left(v + a_n^U \tau_n\right)^2}{2a_n^L} \tag{7-11}$$

As in deceleration case, introducing nominal acceleration and deceleration, we get equation (7-12).

$$s_n^A(v) = v\tau_n + s_n^{jam} + \frac{a_n^a \tau_n^{\,2}}{2} + \frac{v^2}{2a_{n-1}^L} - \frac{\left(v + a_n^a \tau_n\right)^2}{2a_n^d} \tag{7-12}$$

a_n^a : Nominal acceleration rate for vehicle *n*.

Note that the deceleration rate is always less than 0, thus $s_n^{(A)}(v) \geq s_n^{(D)}(v)$ is always satisfied.

7.2.2 A-curve for homogeneous and inhomogeneous traffic

In homogenous traffic, we obtain the following relationship, similar to the deceleration case:

$$s_n^A(v) = \left(1 - \frac{a_n^a}{a_n^d}\right) v\tau_n + s_n^{jam} + \frac{a_n^a \tau_n^{\,2}}{2} - \frac{\left(a_n^a\right)^2}{2a_n^d} \tau_n^{\,2} \tag{7-13}$$

In case of inhomogeneous traffic, e.g., a truck is following an auto, the maximum deceleration value is less than that of the lead vehicle, so the last term in equation (7-12) is growing faster with speed more than in the case of auto-auto or truck-truck pair. Therefore, a truck will need more spacing as the speed increases, and the curve (b) will be bent as in Figure 7-4, which illustrates speed spacing relation for homogeneous flow and auto-truck case. Curve (a) represents A/D curve for the homogeneous case with some arbitrary parameters, and curve (b) for auto-truck case in which following truck's deceleration ability is less than the auto's. Even though curve (b)'s shape is concave, the convexity of

the curve depends on driver characteristics denoted by nominal acceleration, reaction time and maximum deceleration rate as shown in (c), (d) and (e). Curve (c), (d) and (e) each shows the acceleration curve when $a_{n-1}^{L} > a_n^d$, $a_{n-1}^{L} = a_n^d$ and $a_{n-1}^{L} < a_n^d$.

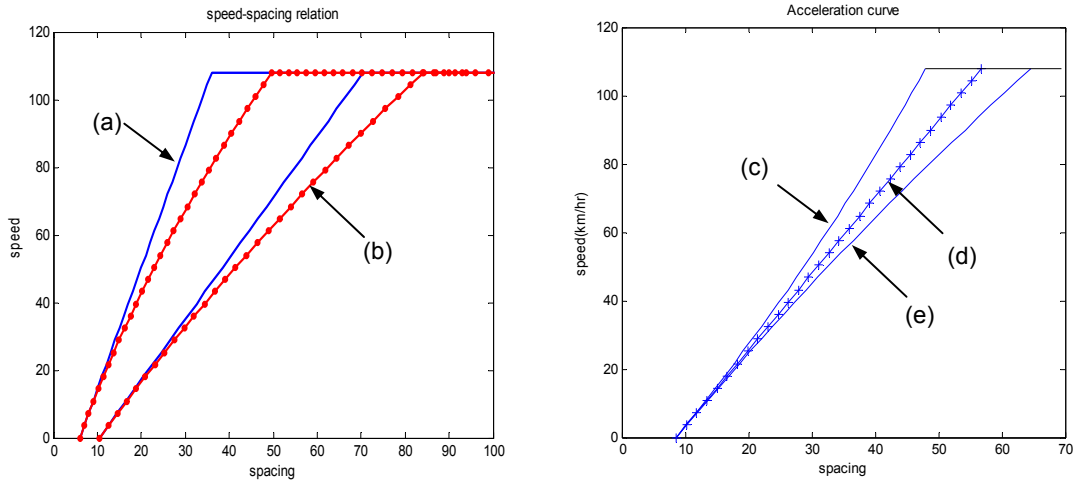

Figure 7-4 Speed spacing relation for acceleration and deceleration

7.2.3 Effects of acceleration capability

It is known that the maximum acceleration is a function of speed. Assume linear relation between speed and nominal acceleration as equation (7-14).

$$a_n^a(v) = \beta a_n^U - \alpha v \tag{7-14}$$

Replacing nominal acceleration with equation (7-14), equation (7-12) gives a new equation (7-15).

$$s_n^A(v) = v\tau_n + s_n^{jam} + \frac{(\beta a_n^U - \alpha v)\tau_n^{\,2}}{2} + \frac{v^2}{2a_{n-1}^L} - \frac{\left(v + (\beta a_n^U - \alpha v)\tau_n\right)^2}{2a_n^d} \tag{7-15}$$

7.2.4 Jam spacing in acceleration phase

From equation (7-13), if the speed is 0, then it gives.

$$s_n^A(0) = s_n^{jam} + \frac{a_n^a \tau_n^{\ 2}}{2} - \frac{\left(a_n^a \tau_n\right)^2}{2a_n^d} \tag{7-16}$$

So the jam density at acceleration phase is

$$s_n^{jam(A)} = s_n^{jam} + \frac{a_n^a \tau_n^{\ 2}}{2} - \frac{\left(a_n^a \tau_n\right)^2}{2a_n^d} \tag{7-17}$$

7.3 Alternative Formulation of the Two Curves

Driver behavior's difference in acceleration and deceleration can be understood by the different sampling time in each case. In braking situation, the spacing is maintained at the minimum level and driver keeps on watching front vehicle to avoid collision, while in the acceleration case, the driver does not need to continually sample the driving situation. Therefore, the reaction time in deceleration situation might be maintained as a minimum value that driver can reach, and the reaction time in acceleration situation is greater because of the less sampling requirement. Thus, by adopting different reaction time and jam spacing for acceleration and deceleration, an alternative simple formulation can be derived:

D-curve Model: $s_n^D(v) = v\tau_n^d + (\frac{1}{2a_{n-1}^L} - \frac{1}{2a_n^d})v^2 + s_n^{jam(d)}$ (7-16)

A-curve Model: $s_n^A(v) = v\tau_n^a + (\frac{1}{2a_{n-1}^L} - \frac{1}{2a_n^d})v^2 + s_n^{jam(a)}$ (7-17)

Where,

Reaction time: $\tau_n^a > \tau_n^d$

Jam spacing: $s_n^{jam(a)} > s_n^{jam(a)}$

a and *d* indicate acceleration and deceleration respectively.

Even with the simplicity, this formula has similar shape with the one derived in the previous section. Therefore, for a practical purpose this simple formula can replace the exact one if used with estimation of parameters.

7.4 Discussion

In this chapter, we derived A-curve and D-curve models describing the fundamental relationship for individual vehicles in stationary conditions. But, actual deceleration or acceleration can start inside the equilibrium region. Considering the speed difference in dynamic situation, for example, if the lead vehicle is slower than the following vehicle, the third term in Equation (7-4) increases and the follower needs a larger spacing for safe driving. So, the driver has to start braking.

$$s_n^D(v) = v_n(t+\Delta t)\tau_n - \frac{\left(v_n(t+\Delta t)\right)^2}{2a_n^L} + \frac{\left(v_{n-1}(t)\right)^2}{2a_{n-1}^L} + s_n^{jam} \tag{7-4}$$

Therefore, the equations developed in this chapter can be applied to determine action points and to make a car-following model. Extracted from simple law of physics directly related to driving, the parameters of the car-following models have physical meaning and the model has less parameters than statistical models which needs numerous parameters without physical meaning. Also, using same approach, we can extend the model to implement the anticipation and maneuvering errors.

In this approach, the shape of the A/D-curve is determined by the relationship between the lead and following vehicles as well as the driver-vehicle characteristics. This implies that the shape of fundamental diagram varies according to vehicle mix. When, the traffic stream consists mostly of passenger cars, the shape of the fundamental diagram is linear.

As the proportion of trucks increases in the traffic stream, the shape of the fundamental diagram can be bent. Therefore, the fundamental diagram varies by location and time with the changes of the vehicle mix.

Chapter 8 Conclusions

8.1 Summary of the Key Findings

The objective of this research is to develop a new traffic theory, which can be used as a framework for developing improved microscopic traffic simulation models. Most of the existing traffic flow theories have been derived from physics laws and cannot explain complicated driving behavior especially in congested traffic. Existing car-following models incorporate numerous parameters that cannot be readily linked with field observations of driver behavior. The approach in this thesis is to analyze in detail the movement and interactions of individual vehicles in congested traffic based on filed data on vehicle trajectories. The analysis provides experimental evidence on the asymmetry in vehicle acceleration and deceleration. A microscopic asymmetric traffic theory is then proposed that can be used to understand and model traffic phenomena.

The main contributions of the thesis can be summarized as follows:

A microscopic asymmetric driving behavior theory is proposed based on detailed analysis of individual vehicle trajectories from the NGSIM database, which is the largest database of vehicle trajectories that exists to date. The findings clearly show the asymmetry in vehicle's acceleration and deceleration, and define five traffic phases: free

flow, acceleration, deceleration, coasting, and stationary. The proposed theory suggests that equilibrium exists in the area bounded by A-curve and D-curve, and provides detailed description and mechanism of phase transitions. Extensions of the basic theory address common driver behavioral characteristics such as maneuvering error and anticipation.

The application of the proposed theory provides reasonable and intuitive explanations verified with experimental data on common traffic phenomena, which cannot be satisfactorily addressed by existing macroscopic or microscopic theories. These phenomena include traffic hysteresis, capacity drop, stability and relaxation following lane change.

The thesis provides a systematic and thorough analysis of the stop-and-go traffic phenomenon, which is critical in modeling congested traffic. The thesis describes in detail the stages and transitions of the generation, growth and dissipation of stop-and-go traffic.

The thesis presents a microscopic fundamental diagram based on the proposed asymmetric theory. This can be used to develop improved car-following models.

8.2 Future Research

Ongoing and future work includes the development and validation of operational microscopic models based on the proposed asymmetry theory. Car-following models can be developed from the A-curve and D-curve equations in Chapter 7, and it can be extended to incorporate dynamic behavior by considering the speed of the lead vehicle. These models can be directly incorporated in operational simulation tools to improve their accuracy in evaluation of performance of existing highway facilities and assessment of operational improvements.

There is a need for understanding lane changing impacts based on experimental data. Lane changing models can be related to car-following models according to the stages of lane changing event: lane changing preparation, lane changing maneuver and relaxation following the lane change. Choice models and gap acceptance models also have to be studied together to develop a comprehensive lane changing model.

Driving behavior is a very complex phenomenon. The proposed theory can be linked to sub-microscopic behaviors considering actual mechanical characteristics of vehicle. By adding more detailed observations, the theory potentially can be extended to sub-microscopic traffic models which deal with detailed driver-vehicle characteristics.

Bibliography

[1] Ahn, S., 2005. Formation and spatial evolution of traffic oscillations. PhD thesis, UC Berkeley.

[2] Ahn, S. and Cassidy, M., 2007. Freeway traffic oscillations and vehicle lane-change maneuvers. Transportation and Traffic Theory 2007.

[3] Banks, J., 1991. Two-capacity phenomenon at freeway bottlenecks: a basis for ramp metering? Transportation Research Record 1320, pp. 83-90.

[4] Brackstone, M. and McDonald, M., 1999. Car-following: a historical review. In Transportation Research Part F 2, pp. 181-196.

[5] Brackstone, M. and et al., 2002. Motorway driver behavior: studies on car following. In Transportation Research Part F 5, pp. 329-344.

[6] Bertini, R.L., 1999. Time dependent traffic flow features at a freeway bottleneck downstream of a merge. PhD. Dissertation, University of California, Berkeley, USA.

[7] Brockfeld, E., Kühne, R.D., Skabardonis, A., and Wagner P., 2003. Toward Benchmark of Microscopic Traffic Flow Models. In Transportation Research Record: Journal of the Transportation Research Board, No. 1852, TRB, National Research Council, Washington, D.C., pp. 124-129.

[8] Cassidy, M.J., 1998. Reproducible bivariate relations in nearly stationary highway traffic. Transportation Research Part B Vol. 32, pp. 49–59.

[9] Cassidy, M.J. and Bertini, R., 1999, Some traffic features at freeway bottlenecks. Transportation Research Part B Vol. 33, pp. 25–42.

[10] Caudill, R.J. and Garrard, W.L., 1977. Vehicle-follower longitudinal control for automated transit vehicles. J. of Dynamic Systems, Measurement, and Control, December, pp. 241-248.

[11] Chung, K., Rudjanakanoknad, J. and Cassidy, M., 2007. Relation between traffic density and capacity at the freeway bottlenecks. Transportation Research Part B Vol. 41, pp. 82-95.

[12] Cohen, S.L., 2004. Application of relaxation procedure for lane changing in microscopic simulation models. In Transportation Research Record: Journal of the Transportation Research Board, No. 1883, TRB, National Research Council, Washington, D.C., pp. 50-58

[13] Daganzo, C.F., 1994. The cell transmission model: A dynamic representation of highway traffic consistent with the hydrodynamic theory. Transportation Research Part B Vol. 28, pp. 269-287.

[14] Daganzo, C.F., 1995. The cell transmission model, part II: Network traffic. Transportation Research Part B Vol. 29, pp. 70-93.

[15] Daganzo, C.F., 1997. Fundamentals of transportation and traffic operations. Pergamon.

[16] Daganzo, C.F., et al. 1999. Possible explanation of phase transitions in highway. Transportation Research Part B Vol. 33, pp. 366-379.

[17] Daganzo, C.F., 2002. A behavioral theory of multi-lane traffic flow. Part II: Merges and the onset of congestion. Transportation Research Part B Vol. 36, pp. 159-169.

[18] Daganzo, C.F., 2006. In traffic flow, cellular automata = kinematic waves. Transportation Research Part B Vol. 40, pp. 396-403.

[19] Del Castillo, J.M., 2001. Propagation of perturbations in dense traffic flow: a model and its implications. Transportation Research Part B Vol. 35, pp. 367-389.

[20] Edie L.C., 1965. Discussion of traffic stream measurements and definitions. Proceedings of The Second International Symposium on The Theory of Road Traffic Flow, London, pp. 139-154.

[21] Foote R.S., 1965. Single lane traffic flow control. Proceedings of The Second International Symposium on The Theory of Road Traffic Flow, London, pp. 84-103.

[22] Forbes, T.W., 1963. Human factor consideration in traffic flow theory, Highway research Record 15, pp. 60-66.

[23] Gipps, P.G., 1981. A behavioural car-following model for computer simulation. Transportation Research Part B Vol. 15, pp. 106-111.

[24] Greenshields, B.D., 1935. A study of traffic capacity, Highway Research Board-National Research Council, Washington DC, pp. 448-477

[25] Hall, F. and Agyemand-Duah, K., 1991. Freeway capacity drop and the definition of capacity. Transportation Research Record 1320, pp 1-98.

[26] Herman, R. and Rothery, R.W., 1965. Propagation of disturbances in vehicular platoons. Vehicular Traffic Science, American Elsevier, New York.

[27] Helbing, D., 1996. Gas-kinetic derivation of Navier-Stokes-like traffic equations. Physical Review E 53(3), pp. 2266-2381.

[28] Hidas, P., 2005. Modelling vehicle interactions in microscopic simulation of merging and weaving. In Transportation Research Part C 13, pp. 37-62.

[29] Kerner, B.S. and Rehborn, H., 1996a. Experimental features and characteristics of traffic jams. Physical Review E Vol. 53, pp. R1297-R1300.

[30] Kerner, B.S. and Rehborn, H., 1996b. Experimental features of complexity in traffic flow. Physical Review E Vol. 53, pp. R4276-R4278.

[31] Kerner, B.S. and Rehborn, H., 1999. Theory of congested traffic flow: self organization without bottlenecks. Proceedings of the 14th International Symposium on Transportation and Traffic Theory, Pergamon, New York, pp. 147–171.

[32] Kerner, B., 2004. Three-phase traffic theory and highway capacity. Physica A 333, pp. 379-440.

[33] Kerner, B., 2005. Microscopic traffic theory and its applications for freeway traffic control, Proceedings of the 16th International Symposium on Transportation and Traffic Theory, Pergamon, New York, pp. 181–203.

[34] Kim, T. and Zhang, H.M., 2004. Gap time and stochastic wave propagation. 2004 IEEE Intelligent Transportation Systems Conference, pp. 88-93.

[35] Kim, T. and Zhang, H.M., 2008. A stochastic wave propagation model. Transportation Research Part B Vol.42, pp. 619-634.

[36] Koshi, M. et al., 1983. Some findings and an overview on vehicular flow characteristics. In: Hurdle,V., Hauer, E., Stuart, G.(Eds), Proceedings of the Eighth International Symposium on Transportation and Traffic Theory. University of Toronto press, Toronto, Canada, pp. 403-451.

[37] Laval, J.A. and Daganzo, C.F., 2003. A hybrid model of traffic flow: impacts of roadway geometry on capacity. TRB 2003 Annual Meeting CD-ROM.

[38] Laval, J.A. and Daganzo, C.F., 2006. Lane-changing in traffic streams, Transportation Research Part B Vol. 40, pp 251-264.

[39] Laval, J.A. and Leclercq, L., 2008. Microscopic modeling of the relaxation phenomenon using a macroscopic lane-changing model. Transportation Research Part B Vol. 42, pp. 511-522.

[40] Laval, J.A., 2008. Hysteresis in the fundamental diagram: impact of measurement methods. International workshop on traffic data collection and its standardization. 2008.

[41] Lighthill, M.J. and Whitham, G.B., 1955. On kinematic waves: II. A theory of traffic flow on long crowded roads. Proceedings of the Royal Society, London, Ser. A 229 1178, pp. 317–345.

[42] Menendez, M., and Daganzo, C. F., 2007. Effects of HOV lanes on freeway bottlenecks. Transportation Research Part B Vol. 41, pp. 809-822.

[43] Nagel, K. and Nelson, P., 2005 A critical comparison of the kinematic wave model with observational data. Transportation and Traffic Theory, Proceedings of the 16th International Symposium on Transportation and Traffic Theory, pp. 145-163.

[44] Newell, G.F., 1965. Instability in dense highway traffic, a review. Proceedings of The Second International Symposium on The Theory of Road Traffic Flow, London, pp. 73-83.

[45] Newell, G.F., 2002. A Simplified car-following theory: a lower order model, Transportation Research Part B Vol. 36, pp. 196-205.

[46] NGSIM, 2006. Next Generation SIMulation. URL: http://ngsim.fhwa.dot.gov/.

[47] Payne, H. J., 1971. Models for Freeway Traffic and Control. Mathematical Models of Public Systems 1, pp. 51-61

[48] Richards, P.I., 1956. Shock waves on the highway. Operations Research 4, pp. 42–51.

[49] Schőnhof, M. and Helbing, D., 2007. Empirical features of congested traffic states and their implications for traffic modeling. Transportation Science 41(2), pp. 135-166.

[50] Transportation Research Board, 2000. Highway Capacity Manual. Washington DC.

[51] Treiber, M., et al., 2005. Delays, Inaccuracies and Anticipation in microscopic traffic models. arXiv: cond-mat/0404736 v3.

[52] Treiber, M., Kesting, A. and Helbing, D., 2006. Understanding widely scattered traffic flows, the capacity drop, and platoons as effects of variance-driven time gaps. Physical Review E 74, 016123.

[53] Treiterer, J. and Myers, J.A., 1974. The hysteresis phenomenon in traffic flow. Proceedings of the sixth International Symposium on Transportation and Traffic Theory, Sydney, Australia, pp.13-38.

[54] Trigs, T. and Harris, W., 1982. Reaction time of drivers to road stimuli. Department of Psychology, Monash University, Australia

[55] Wagner, C., 1998. Asymptotic solutions for a multi-anticipative car-following model, Physica A, pp. 218-224.

[56] Wagner, P.G., 2004. Modelling traffic flow fluctuations. oai: arXiv.org: cond-mat/0411066.

[57] Wiedermann,. R. and Leutzbach, W., 1986. Development and applications of the traffic simulation models at the Institut fur Verhehrwesen. Traffic Engineering and Control, May.

[58] Yeo, H. and Skabardonis, A., 2008. Parameter Estimation for NGSIM Freeway Flow Algorithm, AATT 2008, Greece.

[59] Yeo, H. et al., 2008. The NGSIM Over-Saturated Freeway Flow Algorithm, TRB 2008 Annual Meeting CD-ROM, Paper No. 08-2844.

[60] Zhang, H.M., 1997. A theory of nonequilibrium traffic flow. Transportation Research B Vol. 32, pp. 485–498.

[61] Zhang H.M., 1999. A mathematical theory of traffic hysteresis, Transp. Research Part B Vol. 33, pp. 295–300.

[62] Zhang, H.M., and Kim, T., 2005. A car-following theory for multiphase traffic flow, Transportation Research Part B Vol. 39, pp. 386-399.